RESEARCH MEMORANDUM

EFFECTS OF SEVERAL LEADING-EDGE MODIFICATIONS ON THE STALLING CHARACTERISTICS OF A 45° SWEPT-FORWARD WING

By Gerald M. McCormack and Woodrow L. Cook

Ames Aeronautical Laboratory
Moffett Field, Calif.

NATIONAL ADVISORY COMMITTEE FOR AERONAUTICS

WASHINGTON
June 14, 1949

NATIONAL ADVISORY COMMITTEE FOR AERONAUTICS

RESEARCH MEMORANDUM

EFFECTS OF SEVERAL LEADING-EDGE MODIFICATIONS ON THE STALLING CHARACTERISTICS OF A 45° SWEPT-FORWARD WING

By Gerald M. McCormack and Woodrow L. Cook

SUMMARY

An investigation has been conducted to determine the effects of several leading-edge modifications on the maximum lift and pitching-moment characteristics of a large-scale 45° swept-forward wing.

The results show that, of the modifications tested, a full-span leading-edge flap deflected 30° down gave the largest gain of maximum lift (an increment of 0.22). Use of the full-span leading-edge flap delayed the occurrence of separation to a higher lift coefficient but, in general, the progression and sequence of separation were unchanged. As a result, fore-and-aft shifts of the aerodynamic center occurred which were similar to the shifts of the aerodynamic center of the basic wing. The aerodynamic-center shifts, however, occurred at higher lift coefficients.

The addition of a more highly cambered nose to the airfoil section, which increased the camber of the airfoil from 0.68 to 1.07 percent, increased the maximum lift very little and had little effect on the aerodynamic-center shift.

The use of a leading-edge flap deflected 30° down over the inboard one-half of the wing in combination with a leading-edge flap deflected 10° up over the outboard half increased the maximum lift coefficient approximately the same amount as a half-span leading-edge flap alone. This combination, however, altered the progression of the stall so that only a mild movement of aerodynamic center occurred in contrast to the abrupt shifts that took place with the other configurations.

INTRODUCTION

When operated at moderate and high lift coefficients, highly swept wings, in general, exhibit undesirable aerodynamic characteristics. The underlying causes of these characteristics in the case of a 45° swept-forward wing were discussed in reference 1. It was found that, at a lift coefficient of 0.49, turbulent separation occurred at the trailing edge of the inboard sections and, as the angle of attack was increased, spread outward and forward. This form of separation caused a rearward shift of aerodynamic center and an increase in drag but caused no loss of lift. Before turbulent separation had progressed very far, leading-edge separation occurred over the inboard sections, spreading rapidly outboard as the angle of attack was increased. The effects of leading-edge separation overbalanced the effects of turbulent separation and caused a forward shift of aerodynamic center, great increases in drag, and a decreased lift-curve slope. It also established the maximum lift coefficient of the wing sections and of the entire wing.

In order to obtain satisfactory longitudinal characteristics for the 45° swept-forward wing, as concluded in reference 1, both forms of separation must be postponed to an angle of attack at least as high as the maximum that might be encountered in steady flight. Further, since any evidence of longitudinal instability would possibly curtail the usable lift range, the stall progression, even though it occurs beyond the flight range of angle of attack, should be such that no longitudinal instability results.

As the first step toward improving the stalling characteristics of the 45° swept-forward wing, effort was directed toward delaying and controlling leading-edge separation since it was this form of separation that caused the more deleterious effects. This report presents the results of an investigation conducted in the Ames 40- by 80-foot wind tunnel to determine the effectiveness of several leading-edge modifications intended to delay and control leading-edge separation over the large-scale 45° swept-forward wing.

NOTATION

The data are presented in the form of standard NACA coefficients and symbols which are defined in the following tabulation:

C_L lift coefficient $\left(\frac{\text{lift}}{qS}\right)$

c_l section lift coefficient $\left(\frac{\text{lift per unit span}}{qc}\right)$

C_D drag coefficient $\left(\frac{\text{drag}}{qS}\right)$

C_m pitching-moment coefficient computed about the quarter-chord point of the mean aerodynamic chord $\left(\frac{\text{pitching moment}}{qS\bar{c}}\right)$

a.c. aerodynamic center measured in percent chord aft of the leading edge of the mean aerodynamic chord

P pressure coefficient $\left(\frac{p_l - p}{q}\right)$

p free-stream static pressure, pounds per square foot

p_l local static pressure, pounds per square foot

q free-stream dynamic pressure, pounds per square foot

S wing area, square feet

a mean line designation

b wing span, feet

$\bar{c}$ mean aerodynamic chord $\left(\frac{\int_0^{b/2} c^2 dy}{\int_0^{b/2} c\, dy}\right)$, feet

c local chord, feet

x chordwise coordinate parallel to plane of symmetry, feet

y spanwise coordinate perpendicular to plane of symmetry, feet

α angle of attack of chord plane of basic wing, degrees

δ_n angle of deflection of leading-edge flap, positive downward, degrees

MODEL, TESTS, AND RESULTS

The geometric characteristics of the swept-forward wing are shown in figure 1. The wing had 45° of sweep forward of the quarter-chord line, an aspect ratio of 3.55, a taper ratio of 0.5, no twist, and no dihedral. The wing sections were constant across the span, and were NACA 64_1A112 sections perpendicular to the quarter-chord line. A photograph of the wing mounted in the wind tunnel is shown in figure 2.

The wing was equipped with a plain leading-edge flap. (See fig. 3.) This flap was hinged about the 12.5-percent-chord line (of sections perpendicular to the quarter-chord line) on the lower surface of the wing when deflected downward, and was hinged about the 16-percent-chord line on the upper surface of the wing when deflected upward. (The hinge lines on the upper and lower surfaces were different due to structural reasons.) When the leading-edge flap was deflected, the transition surface between the flap and the wing had a radius of curvature equal to the radius from the hinge line.

After tests of the wing equipped with the leading-edge flaps were completed, the wing was fitted with a nose piece which incorporated more camber than the original 64_1A112 section. (See fig. 3.) The lines of the cambered nose were obtained from the forward 12.5 percent of a 64_1-012 thickness distribution combined with an $a = 1.0$ mean line which was cambered for an ideal lift coefficient of 2 (that is, an NACA 64-2012 section). This nose piece was fitted so that both the upper surface and the lower surface became tangent to the contour of the main portion of the wing at 12.5-percent chord.

Pressure orifices were positioned over the upper and lower surfaces of streamwise sections which were located at 28.1-percent, 57.4-percent, and 85.0-percent semispan. The chordwise locations are given in table I.

Force and pressure-distribution measurements were made through an angle-of-attack range at zero sideslip. The data were obtained at approximately 110 miles per hour (Reynolds number of 10.6×10^6 based on the mean aerodynamic chord length of 10.41 ft). The data were obtained at one value of Reynolds number, since data obtained on the plain wing (reference 1) showed no significant Reynolds number effects, particularly within the purpose of this report.

An index to the test results is given in the following tabulation:

Figure No.	Configuration	Results Shown
4	Wing with full-span leading-edge flaps	C_D, α, C_m vs C_L
5	Wing with leading-edge flaps of varying spanwise extent	Do.
6	Wing with inboard one-half span leading-edge flap deflected down, outboard one-half span leading-edge flap deflected up	Do.
7	Wing with cambered nose of varying spanwise extent	Do.
8	Wing with full-span leading-edge flaps	Chordwise Pressures
9	Wing with inboard one-half span leading-edge flap deflected down, outboard one-half-span leading-edge flap deflected up	Do.
10	Wing with full-span cambered nose	Do.

Standard tunnel-wall corrections for a straight wing of the same area and span as the swept-forward wing have been applied to the angle-of-attack and drag-coefficient data. This procedure was followed since a brief analysis indicated that tunnel-wall corrections were approximately the same for straight and swept wings of the size under consideration. The corrections applied are as follows:

$$\Delta\alpha = 0.74\ C_L$$

$$\Delta C_D = 0.013\ C_L^2$$

The data were corrected for drag tares. Pitching-moment tares were not applied since they were not known with sufficient accuracy to warrant application. Indications are that they are not of sufficient magnitude to materially affect the results.

DISCUSSION

As previously mentioned, in the endeavor to attain satisfactory longitudinal characteristics for the swept-forward wing, effort was first directed toward controlling the leading-edge type of separation. This was taken as the first step in spite of the fact that turbulent separation occurred prior to leading-edge separation. It was felt that any alleviation of the effects of turbulent separation that might be obtained would have little influence on leading-edge separation. Hence, the effects of leading-edge separation would soon overshadow any beneficial effects obtained in the trailing-edge separation pattern. On the other hand, it was reasonable to expect that beneficial changes of the leading-edge flow would be reflected by beneficial changes in the trailing-edge flow. In order to control leading-edge separation the peak suction pressure must be decreased since the magnitude and the gradient of the pressure recovery appear to be the principal factors causing separation. The devices used to lower the suction peak on the swept-forward wing were a plain leading-edge flap and increased camber in the forward portion of the wing.

Plain Leading-Edge Flaps

Full-span flaps.- The longitudinal characteristics of the swept-forward wing equipped with a full-span plain leading-edge flap are shown in figure 4. Compared to the basic wing, the linear portion of the lift curve was extended from a lift coefficient of 0.65 to 0.87 (an increment of 0.22) and the maximum lift was increased from 1.04 to 1.26 (an increment of 0.22). Drag coefficients in the moderate-lift range were significantly reduced. The first break of the pitching-moment curve (rearward shift of aerodynamic center) was delayed from a lift coefficient of 0.49 to 0.76 (an increment of 0.27); the second break (forward shift of aerodynamic center) was delayed from 0.75 to about 0.93 (an increment of 0.18).

Although the full-span leading-edge flaps delayed the occurrence of separation, allowing attainment of higher maximum lift and increasing the lift coefficients at which irregularities appeared in the force characteristics, they had essentially no effect on the progression of stall. This was indicated by the large, abrupt shifts of aerodynamic center which were encountered once separation had occurred. The progression of the stall can more easily be seen by examination of the pressure distributions. In figure 11, comparisons can be made between the pressure distributions at the 28.1-percent-semispan station for the basic wing and for the wing with the full-span leading-edge flaps. The distributions at that semispan station are typical of all distributions

obtained. It can be seen in figure 11(a) that, on the basic wing, starting at about 12.5° angle of attack, the pressures failed to recover over the trailing edge, while the growth of pressures over the leading edge was little affected. This, as described in reference 1, indicated that turbulent separation was taking place. When the leading-edge flap was deflected the same changes in pressure distribution occurred but were delayed to about 16.6° angle of attack. Thus, the leading-edge flap delayed the occurrence of turbulent separation approximately 4°. The chordwise redistribution of load resulting from turbulent separation caused a negative increment of pitching moment ($\Delta C_m = -0.03$) of essentially the same magnitude as the increment associated with the basic wing.

Within a short angle-of-attack range after the onset of turbulent separation, leading-edge separation occurred over the inboard sections of both the basic wing and the wing with the leading-edge flap. The resulting changes in the pressure distributions can be seen in figure 11(b). On the basic wing the suction peak began to decrease at about 16.6° angle of attack. This, as described in reference 1, indicated that leading-edge separation was taking place. When the leading-edge flap was deflected, two suction peaks occurred: one over the hinge line, due to camber; the other at the leading edge, due to angle of attack. The suction peak over the hinge line began to decrease at about 20.8° angle of attack. This caused a decrease of slope of the section lift curve but did not define the maximum lift of the section. Section lift continued to increase until the suction peak at the leading edge began to decrease at about 24.9° angle of attack. Beyond this angle of attack the section began to lose lift. This loss of lift occurred first over the inboard sections, and, as angle of attack was further increased, occurred over sections farther outboard.

The decreased section lift-curve slope resulting from loss of the suction peak over the hinge line caused an outward, hence, forward shift of the spanwise center of load. This, in turn, caused a forward shift of the aerodynamic center similar to that which occurred on the basic wing. On the wing with leading-edge flap, the aerodynamic center moved forward to about the 7-percent point of the mean aerodynamic chord in the high lift range; whereas on the basic wing it moved to a point 11 percent of the mean aerodynamic chord forward of the leading edge. The lesser movement in the case of the flapped wing is attributable to the fact that lift was not lost suddenly as it was in the case of the basic wing, but instead occurred over a range of angles of attack extending from the angle at which the suction peak over the hinge line began to decrease to the angle at which the suction peak at the leading edge began to decrease.

There are little two-dimensional data available on which to predict the benefits obtainable by deflecting a plain leading-edge flap. It is of considerable interest, however, to compare such two-dimensional

results that are available with swept-wing results. The effect of deflecting a leading-edge flap on an NACA 0009 airfoil in two-dimensional flow at a Reynolds number of 1.2×10^6 is given in reference 2. Leading-edge separation was delayed to the extent that an increment of maximum lift coefficient of about 0.55 was obtained. Similar to the swept-forward wing, however, the maximum lift coefficient was still limited by the leading-edge type of separation. Thus, it is reasonable to make a comparison between the two cases. The two-dimensional value, when corrected for the effects of sweep,[1] is equivalent to an increment of maximum lift coefficient of about 0.27 on a 45° swept wing. On the swept-forward wing (64_1A112 section perpendicular to the quarter-chord line), a maximum-lift increment of 0.22 was obtained using the full-span leading-edge flap. The two values agree reasonably well, indicating that the effects of a leading-edge flap on swept-wing characteristics can be approximated by using simplified sweep theory (reference 3) to correct two-dimensional data.

Partial-span flaps.- In an attempt to lessen the forward shift of aerodynamic center which was still present with the full-span leading-edge flaps, the spanwise extent (from the center line outward) of the leading-edge flap was varied. By this means it was intended to delay leading-edge separation over the inboard sections (relative to the basic wing) without appreciably changing that over the outboard sections. Thereby the progressive outward and forward shift of center of load would be lessened and the forward movement of aerodynamic center would be decreased.

The longitudinal characteristics of the wing with leading-edge flaps of various spans are shown in figure 5. It is seen that the beneficial effects of the leading-edge flap were in all cases directly dependent upon the span of the flap. The greater the span of the flap the greater were the reductions in drag, and the smaller were the shifts of aerodynamic center, particularly the forward shift, and the higher were the increases in maximum lift. Thus the partial-span leading-edge flap did not change the progression of stall as anticipated. This

[1] In accordance with the concepts of Betz (reference 3), on an oblique wing, only the velocity component normal to the quarter-chord line influences the pressures over the wing. Thus, on an oblique wing, since the dynamic pressure perpendicular to the quarter-chord line will decrease in proportion to the square of the cosine of the angle of sweep, the maximum lift coefficient of the section should also decrease in proportion to the square of the cosine of the angle of sweep.

ineffectiveness was shown by the pressure distributions to be due to the disturbing effect on the flow of the discontinuity at midspan between the deflected and undeflected portions of the flap. This discontinuity caused an earlier stall over the inboard part of the wing thus negating any beneficial effects that might have been obtained.

Differentially deflected flaps.— A further attempt was made to modify the sequence of separation in the effort to improve the longitudinal stability of the wing by deflecting the inboard half semispan of the leading-edge flap downward 30° and the outboard half semispan of the leading-edge flap upward 10°. Thereby, it was anticipated that, while the down-deflected flap would delay the stall over the inboard area, the up-deflected flap would cause the outboard area to stall at an earlier angle of attack. The longitudinal characteristics of the wing with this configuration are shown in figure 6. It is evident that considerably less shift of aerodynamic center was encountered with this configuration than with the full-span leading-edge flap. This is further shown by a comparison of the aerodynamic center travel of the various configurations in the following tabulation:

Configuration	Position of a.c. at low C_L (percent $\bar{c}$)	Approx. aft position of a.c. (percent $\bar{c}$)	Approx. forward position of a.c. (percent $\bar{c}$)	Maximum a.c. movement (percent $\bar{c}$)
A	30	41	-11	52
B	25	53	7	46
C	29	59	-11	70
D	28	28	16	12

Note:
A. Basic wing
B. Wing with full-span leading edge flap deflected 30° down
C. Wing with inboard one-half-span leading-edge flap deflected 30° down
D. Wing with leading-edge flap with inboard one-half span deflected 30° down and outboard one-half span deflected 10° up

The large diminution of aerodynamic-center travel obtained by differential deflection of the leading-edge flap is desirable from the longitudinal-stability standpoint. It should be noted, however, that, compared to the full-span leading-edge flap, the drag rise was very rapid and some loss of lift was sustained.

Cambered Nose

The longitudinal characteristics of the wing equipped with a full-span and an inboard half-span cambered nose are shown in figure 7. Although slight gains were evidenced, the over-all effect of the cambered nose on the wing characteristics was insignificant.

The reason for this can be seen upon examination of the pressure distributions. Examples of the pressure distributions over the upper surface of streamwise sections at 28.1 percent of the semispan of the basic wing, the wing with cambered nose, and the wing with leading-edge flap deflected 30° are compared in figure 12. It can be seen in figure 12(a) that, compared to the plain wing, the suction peak and the recovery gradient obtained over the wing with cambered nose were decreased. It is of interest to compare these changes in pressure distributions with the changes which would be theoretically predicted. Pressure distributions for the three configurations tested computed in accordance with the methods of reference 4 are shown in figure 12(b). It is seen that the nature of the changes to be expected by modifying the airfoil contour are indicated qualitatively by the theoretical pressure distributions.

The changes in the pressure distribution obtained by using the cambered nose were not sufficient to significantly alter the separation characteristics. This was indicated by the small changes evidenced in the force data. The information is not available to determine how much the pressure distribution must be changed, that is, how much camber should be incorporated to appreciably delay separation. The airfoil was composed of the forward 12-1/2 percent of a very highly cambered airfoil (64_1-012 cambered for an ideal lift coefficient of 2) combined with the aft 87-1/2 percent of the original 64_1A112 airfoil. The result was a maximum mean line camber of 1.07 percent of chord located at approximately 12-1/2 percent chord. This was considerably more than the camber of the 64_1A112 airfoil (which had a maximum camber of 0.68 percent of chord located at 50-percent chord) but was far less than the wing equipped with the leading-edge flap deflected 30° (which had a maximum camber of 7.04 percent of chord located at 12-1/2-percent chord). As a further comparison, an NACA 4412 airfoil which stalls from progressive turbulent separation (the kind of stall desired) has a maximum mean line camber of 4 percent of chord located at approximately 40-percent chord. Judging from the foregoing, the indications are that a cambered nose should have four or five times the amount of camber used in the present tests to significantly alter the stalling characteristics of the wing.

CONCLUDING REMARKS

The results of the tests made to improve the maximum lift and the longitudinal characteristics of a 45° swept-forward wing by using leading-edge modifications are summarized in the following table:

Configuration	$C_{L_{max}}$	$\Delta C_{L_{max}}$	Position of a.c. at low C_L (percent $\bar{c}$)	C_L at which a.c. moved aft	Approx. aft position of a.c. (percent $\bar{c}$)	C_L at which a.c. moved forward	Approx. forward position of a.c. (percent $\bar{c}$)
A	1.04	--	30	0.49	41	0.75	-11
B	1.26	.22	25	.76	53	.93	7
C	1.18	.14	29	.76	59	.94	-11
D	1.14	.10	28	none	28	.63	16
E	1.05	.01	30	.53	41	.78	-23

Note:
A. Basic wing
B. Wing with full-span leading-edge flap deflected 30° down
C. Wing with inboard one-half span leading-edge flap deflected 30° down
D. Wing with leading-edge flap with inboard one-half span deflected 30° down and outboard one-half span deflected 10° up
E. Wing with full-span cambered nose

Insofar as maximum lift is concerned, the greatest gain was obtainable by using a full-span leading-edge flap deflected 30° down. Use of the leading-edge flap delayed separation, but, in general, the progression and sequence of separation were unchanged. The fore-and-aft shifts of aerodynamic center of the plain wing, therefore, were also associated with the wing with leading-edge flap. The aerodynamic center shifts were, however, evidenced at higher lift coefficients as indicated in the table.

Adding a more highly cambered nose to the airfoil section, which increased the camber from 0.68 to 1.07 percent of the chord, increased the maximum lift very little and had little effect on the aerodynamic-center shift.

The use of a leading-edge flap deflected 30° down over the inboard one-half of the wing in combination with a leading-edge flap deflected 10° up over the outboard half increased the maximum lift coefficient approximately the same amount as the inboard half-span leading-edge flap deflected 30° down. This combination, however, altered the progression of the stall so that only a mild movement of aerodynamic center occurred without the abrupt shifts that took place with the other configurations.

Ames Aeronautical Laboratory,
National Advisory Committee for Aeronautics,
Moffett Field, Calif.

REFERENCES

1. McCormack, Gerald M., and Cook, Woodrow L.: A Study of Stall Phenomena on a 45° Swept-Forward Wing. NACA TN 1797, 1949.

2. Lemme, H. G.: Kraftmessungen und Druckverteilungsmessungen an einem Flügel mit Knicknase, Vorflügel, Wolbungs- und Spreizklappe. Aerodynamische Versuchsanstalt Göttingen E. V. Forschungsbericht Nr. 1676. Oct. 15, 1942.

3. Betz, A.: Applied Airfoil Theory. Unsymmetrical and Non-Steady Types of Motion. Vol. IV of Aerodynamic Theory, div. J, Ch. IV, sec 4, W. F. Durand, ed., Julius Springer (Berlin), 1935, pp. 94-107.

4. Allen, H. J.: General Theory of Airfoil Sections Having Arbitrary Shape or Pressure Distribution. NACA Rep. 833, 1945.

TABLE I

CHORDWISE ORIFICE POSITION AT STATIONS 28.1-PERCENT, 57.4-PERCENT, AND 85.0-PERCENT SEMISPAN

Orifice No.	Wing with leading-edge flap deflected 30° down		Wing with cambered nose		Wing with leading-edge flap deflected 10° up	
	Upper surface (percent chord)	Lower surface (percent chord)	Upper surface (percent chord)	Lower surface (percent chord)	Upper surface (percent chord)	Lower surface (percent chord)
1	0	- - -	0	- - -	0	- - -
2	.06	0.38	.41	0.41	.31	0.2
3	.23	.67	.66	.66	.58	.43
4	.58	1.22	.91	.91	1.10	.89
5	1.00	1.75	1.16	1.16	1.62	1.36
6	1.82	2.79	1.67	1.67	2.65	2.23
7	2.66	3.80	2.16	2.16	3.68	3.28
8	3.95	5.29	3.16	3.16	5.19	4.73
9	6.14	7.74	4.16	4.16	7.72	7.16
10	8.36	10.17	5.67	5.67	15.00	9.62
11	10.75	15.00	8.16	8.16	20.00	15.00
12	13.25	20.00	10.67	10.67	30.00	20.00
13	15.00	30.00	15.00	15.00	40.00	30.00
14*	15.88	40.00	20.00	20.00	50.00	40.00
15	20.00	50.00	30.00	30.00	60.00	50.00
16	30.00	60.00	40.00	40.00	70.00	60.00
17	40.00	70.00	50.00	50.00	80.00	70.00
18	50.00	80.00	60.00	60.00	90.00	80.00
19	60.00	90.00	70.00	70.00	97.50	90.00
20	70.00	97.50	80.00	80.00	- - -	97.50
21	80.00	- - -	90.00	90.00	- - -	- - -
22	90.00	- - -	97.50	97.50	- - -	- - -
23	97.50	- - -	- - -	- - -	- - -	- - -

*No orifice no. 14 station 28.1-percent semispan on the upper surface on leading-edge flap deflected 30° down.

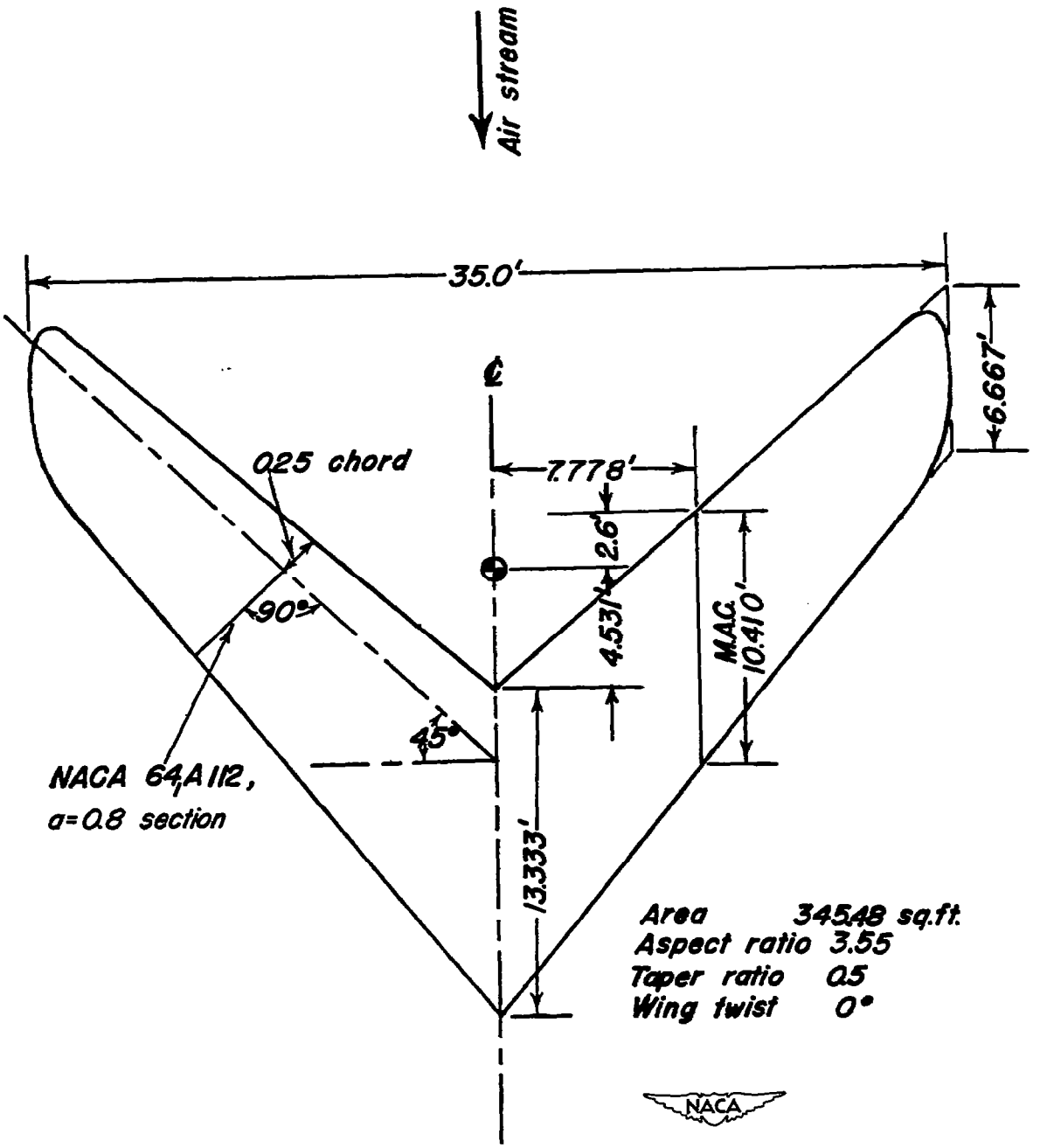

Figure 1.- Geometric characteristics of 45° swept-forward wing.

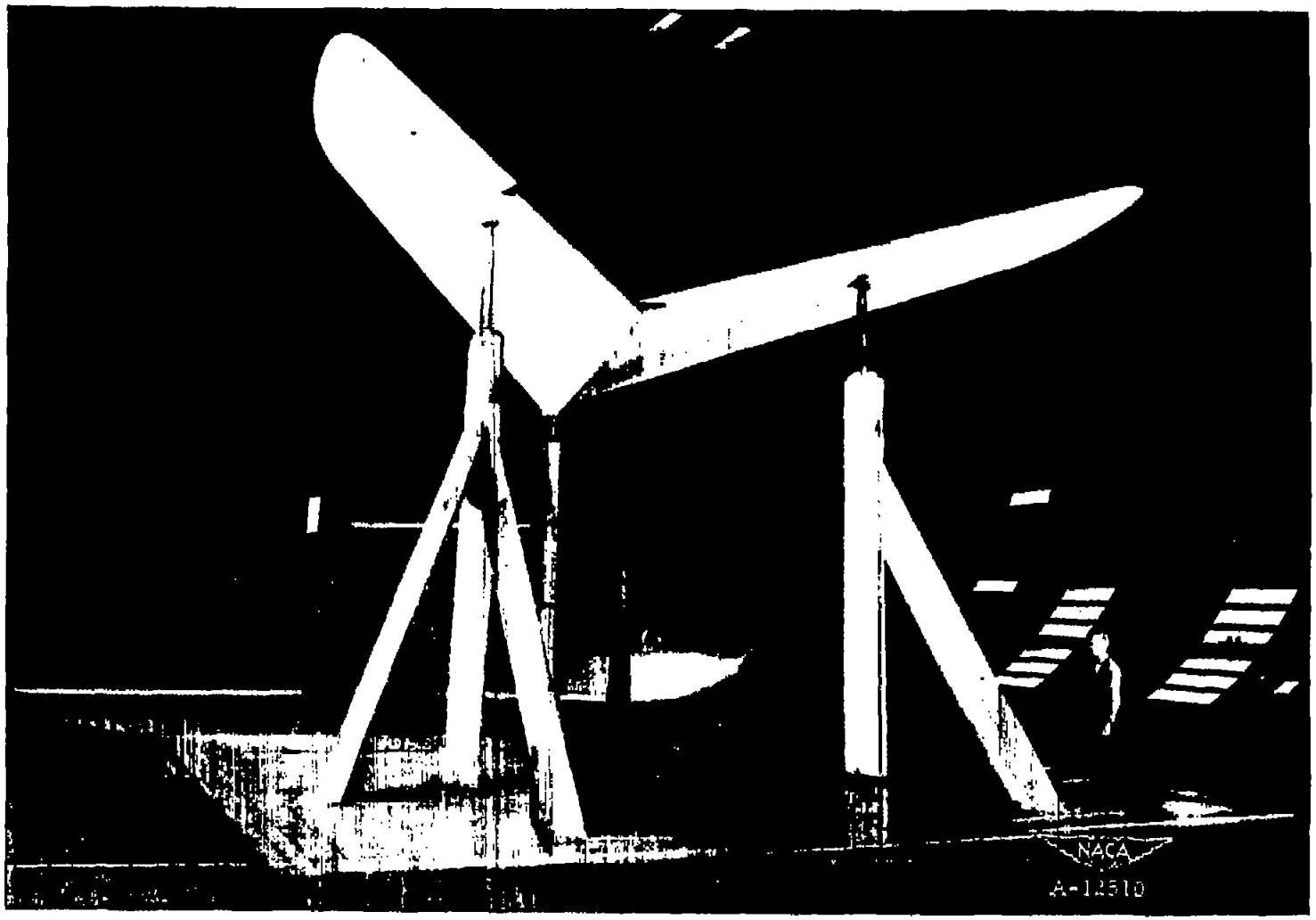

Figure 2.– The 45° swept-forward wing in the Ames 40- by 80-foot wind tunnel. Inboard one-half-span leading-edge flap deflected down.

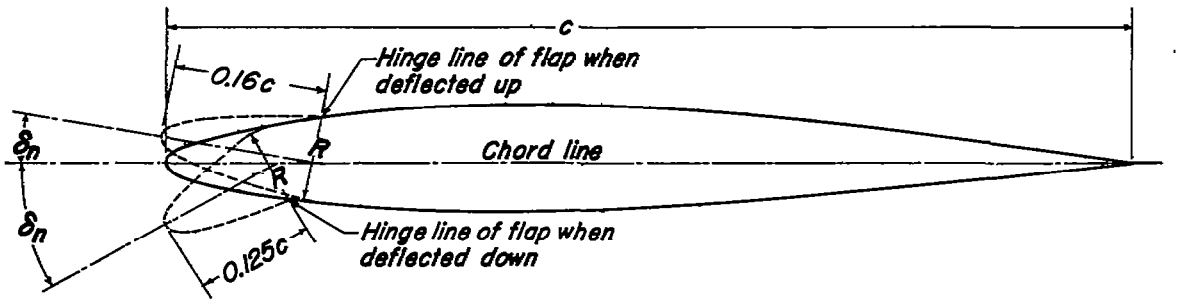

Wing section with leading-edge flap

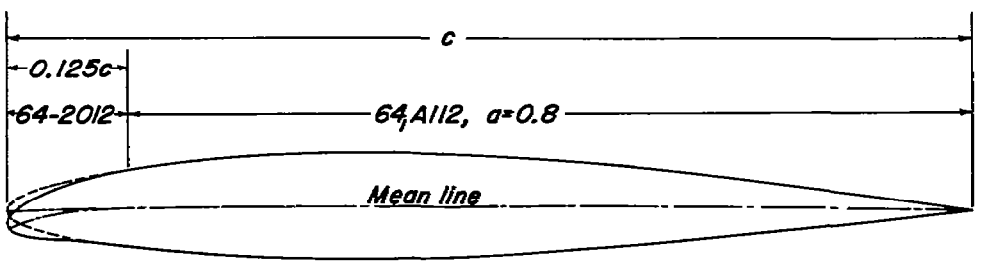

Wing section with cambered nose

NACA

Figure 3.- Sketch of wing sections tested on 45° swept-forward wing.

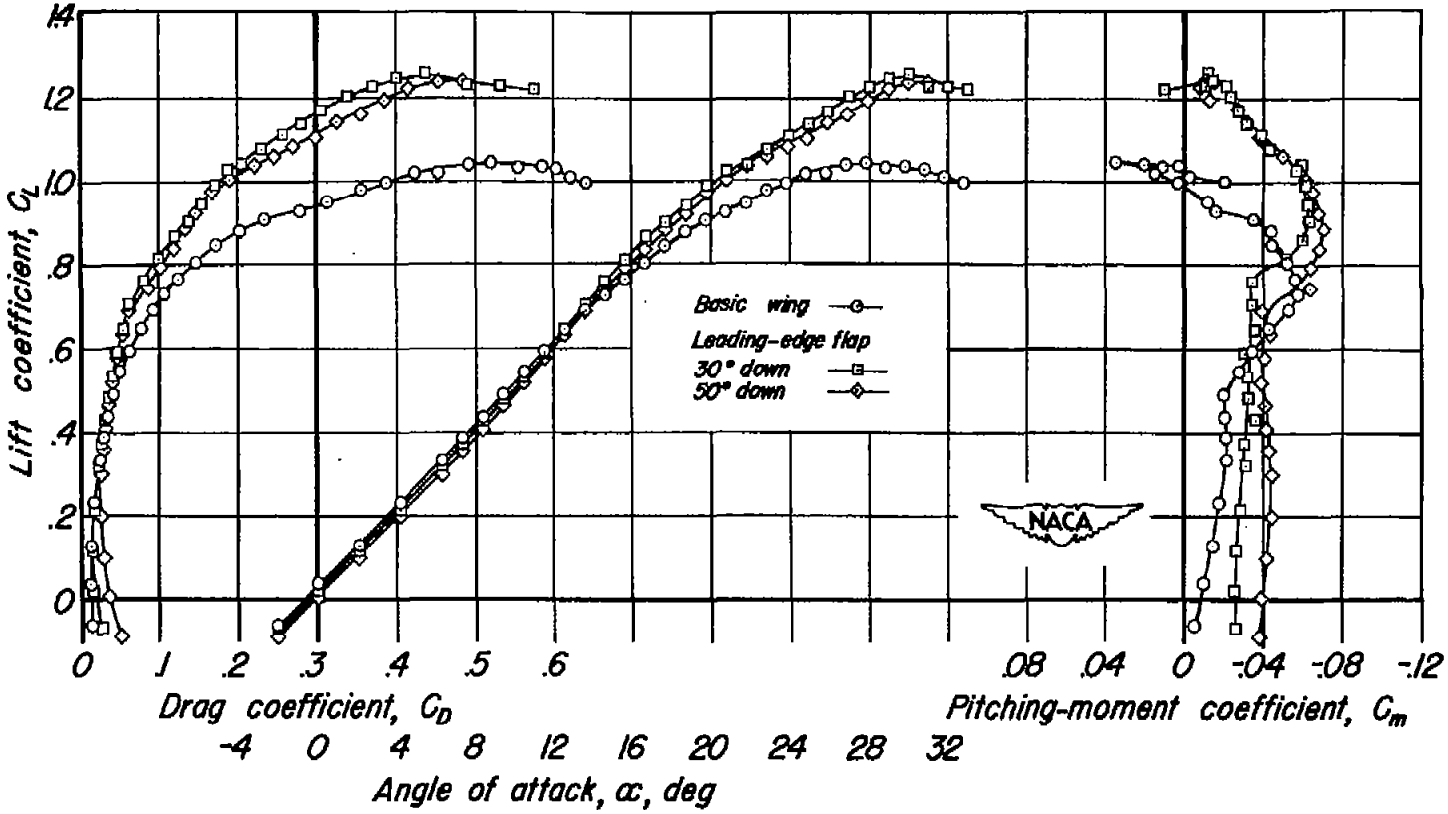

Figure 4.—Longitudinal characteristics of the 45° swept-forward wing with a full-span leading-edge flap deflected down to various angles.

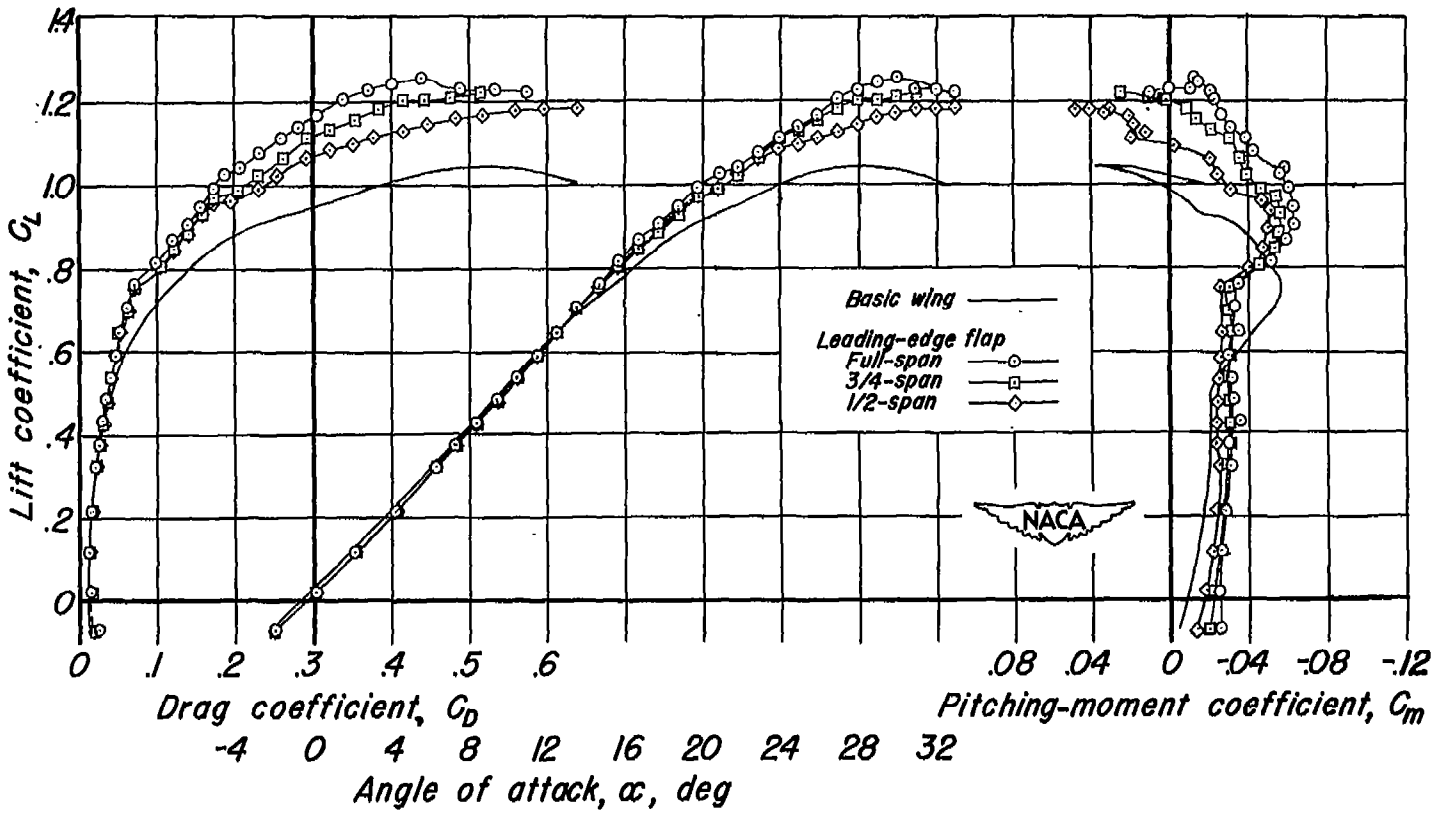

Figure 5.— Longitudinal characteristics of the 45° swept-forward wing with a leading-edge flap of varying spanwise extent deflected 30° down.

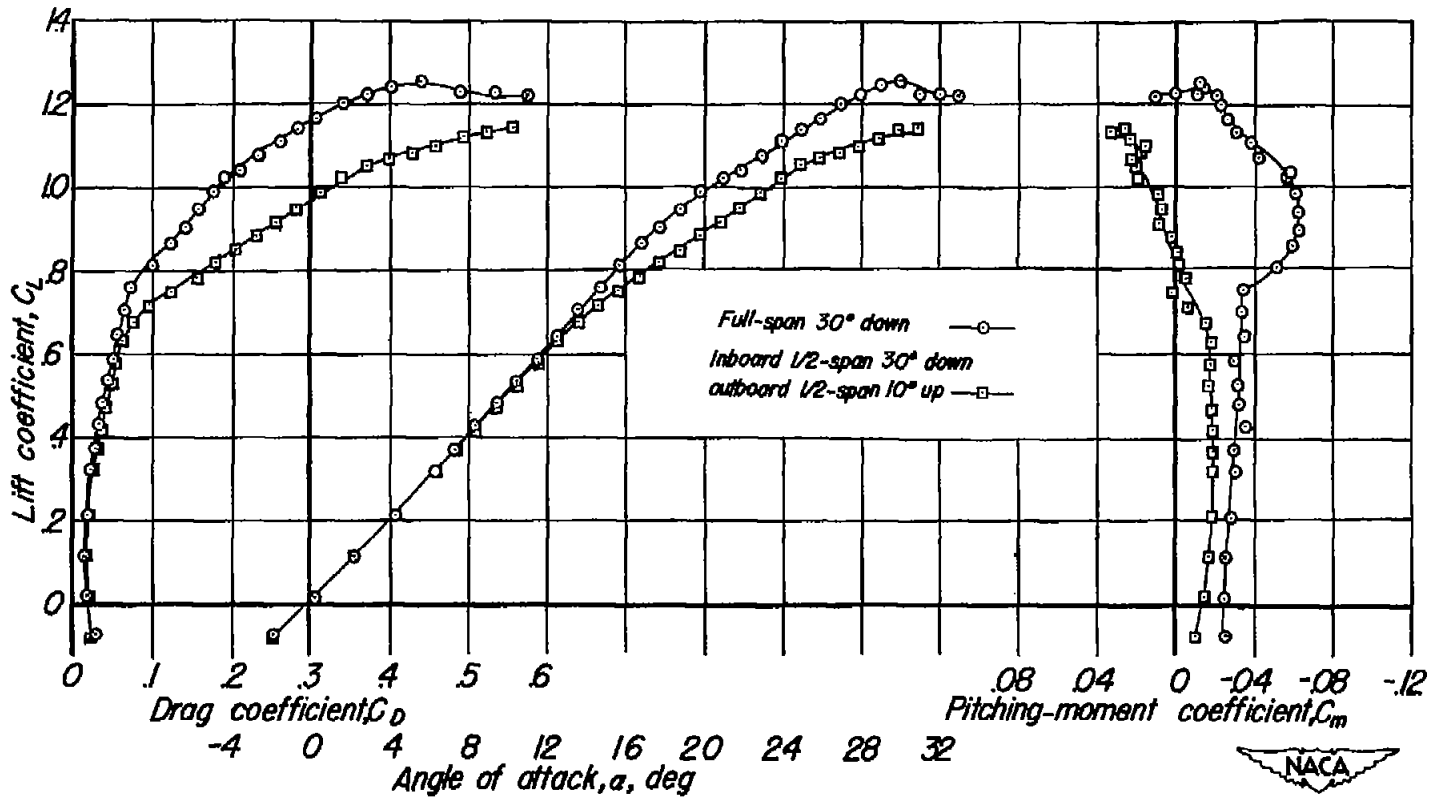

Figure 6. — Longitudinal characteristics of the 45° swept-forward wing with the inboard half-span of the leading-edge flap deflected down and the outboard half-span of the leading-edge flap deflected up.

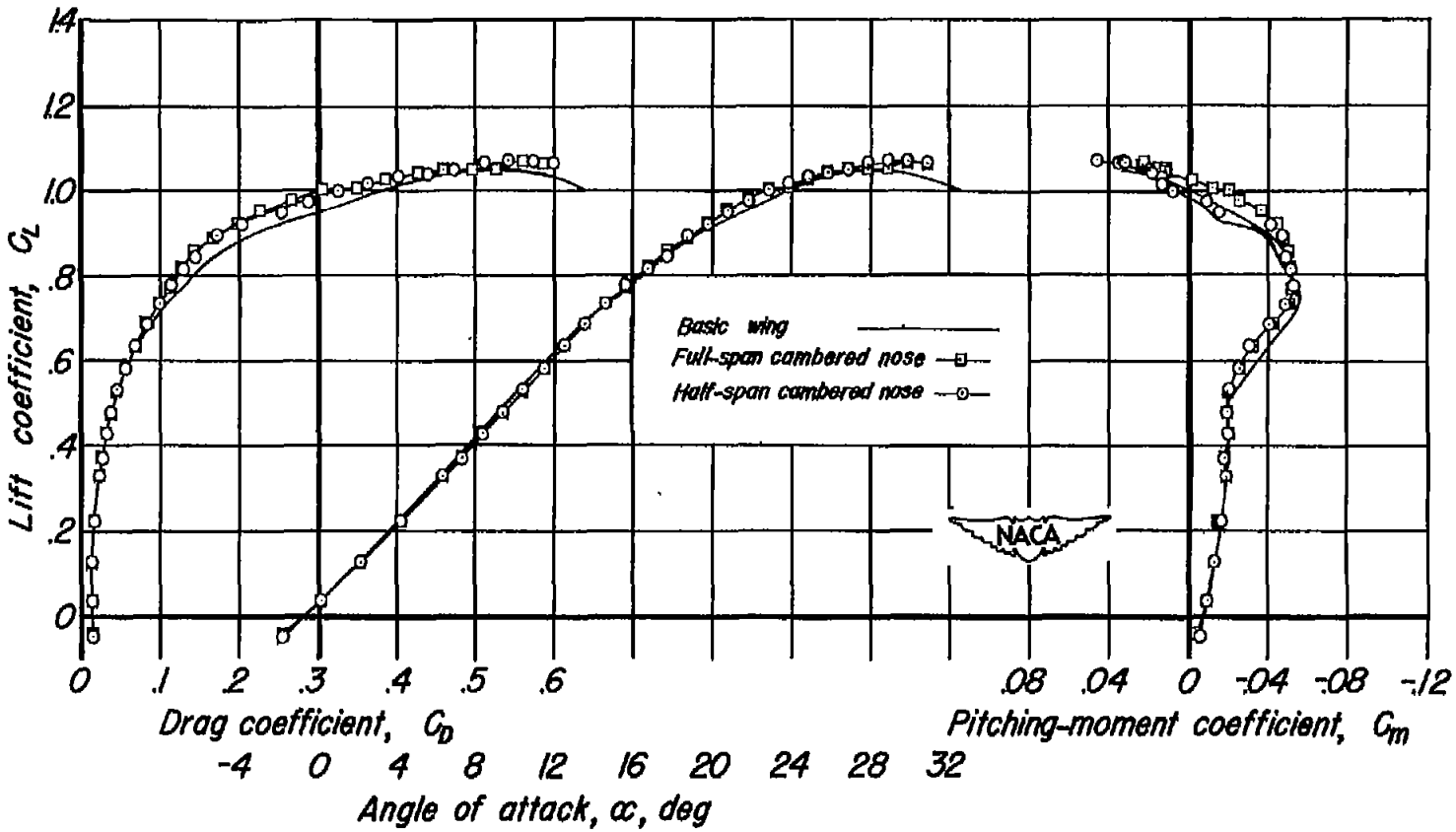

Figure 7.—Longitudinal characteristics of the 45° swept-forward wing with a full-span and half-span cambered nose.

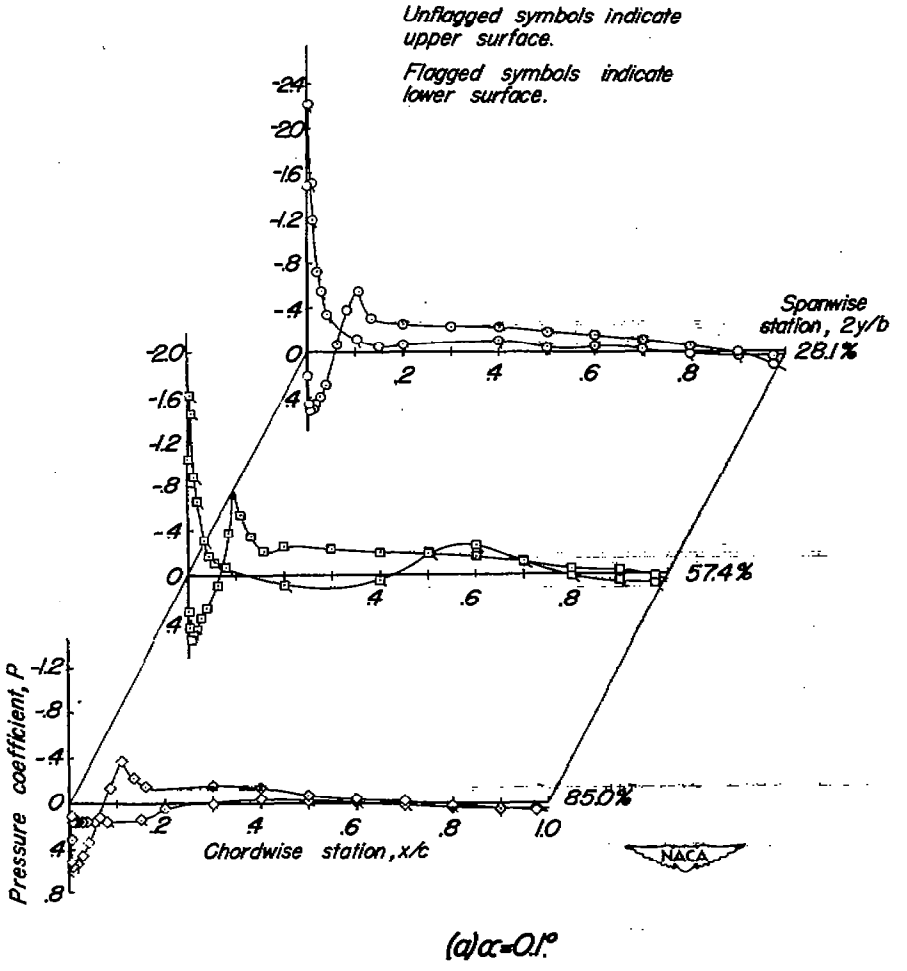

(a) $\alpha = 0.1°$

Figure 8. —Chordwise pressure distributions for 45° swept-forward wing with a full-span leading-edge flap deflected 30° down.

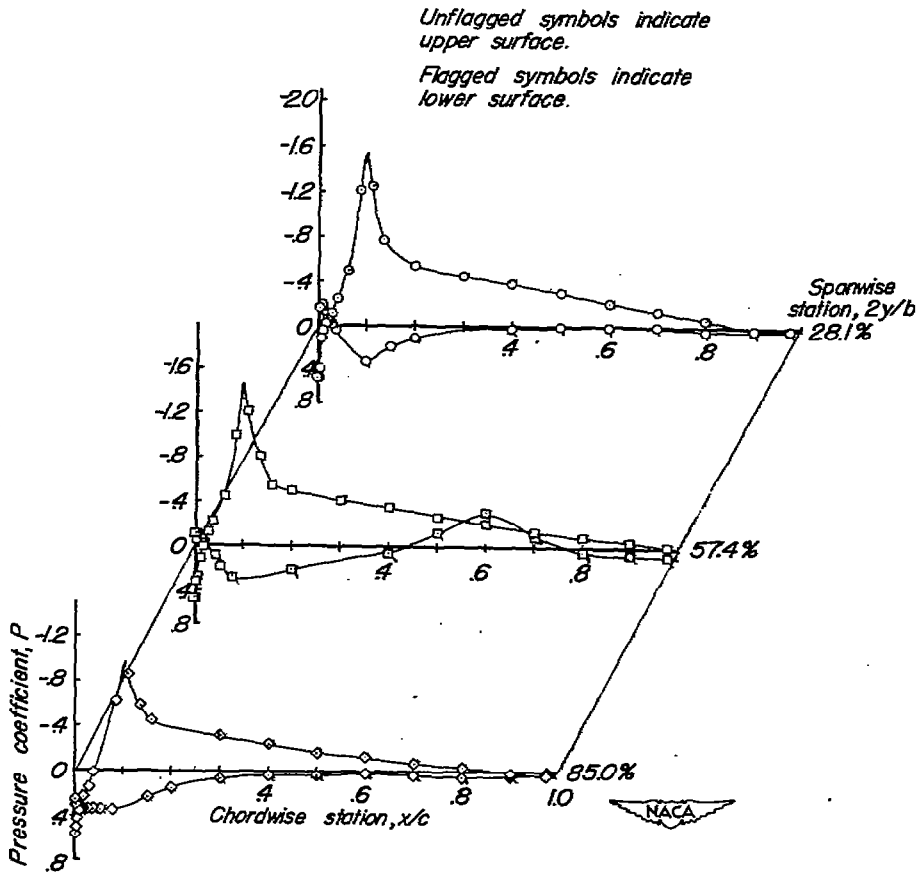

(b) α=6.3°.

Figure 8.–Continued.

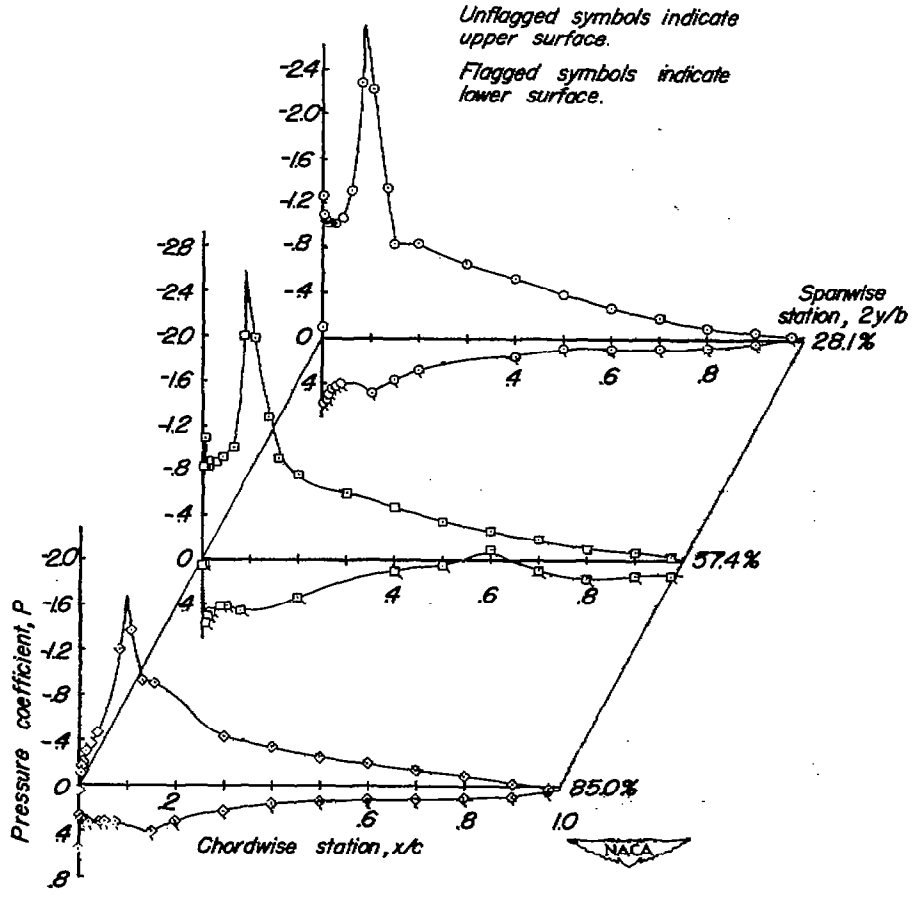

(c) $\alpha = 12.5°$.

Figure 8. –Continued.

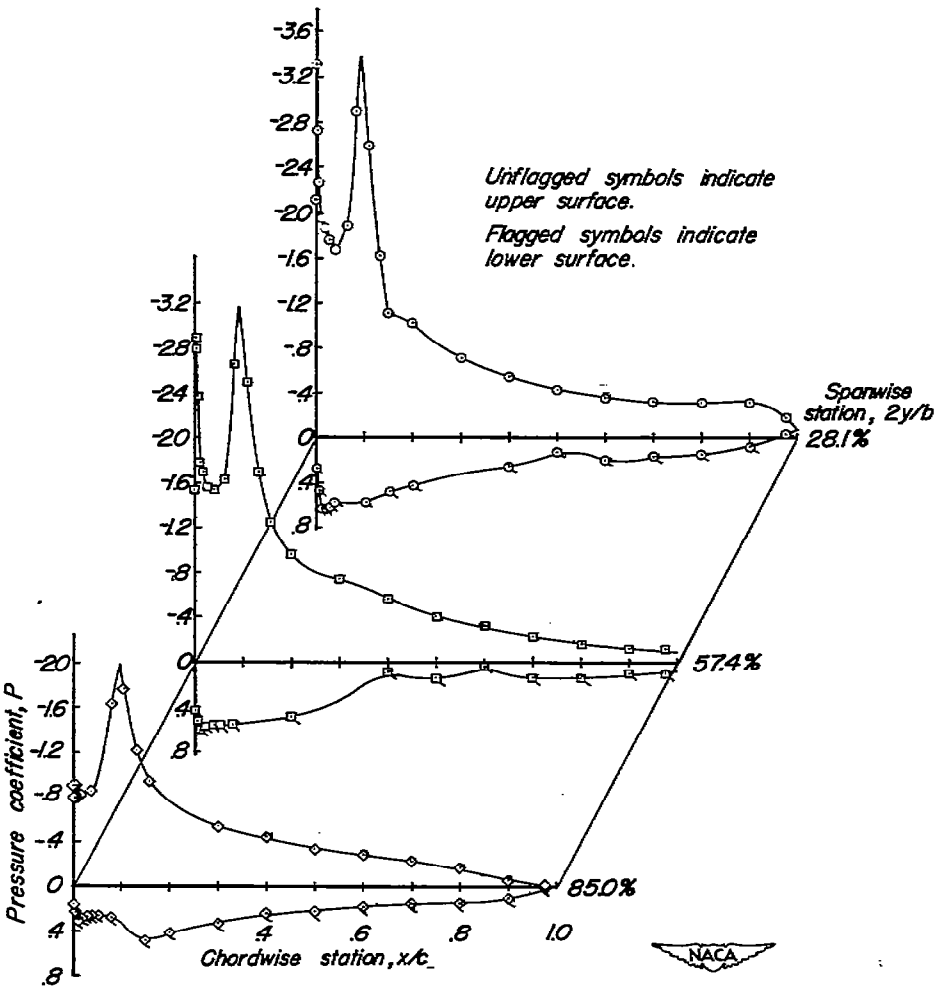

(d) $\alpha = 16.6°$.

Figure 8. – Continued.

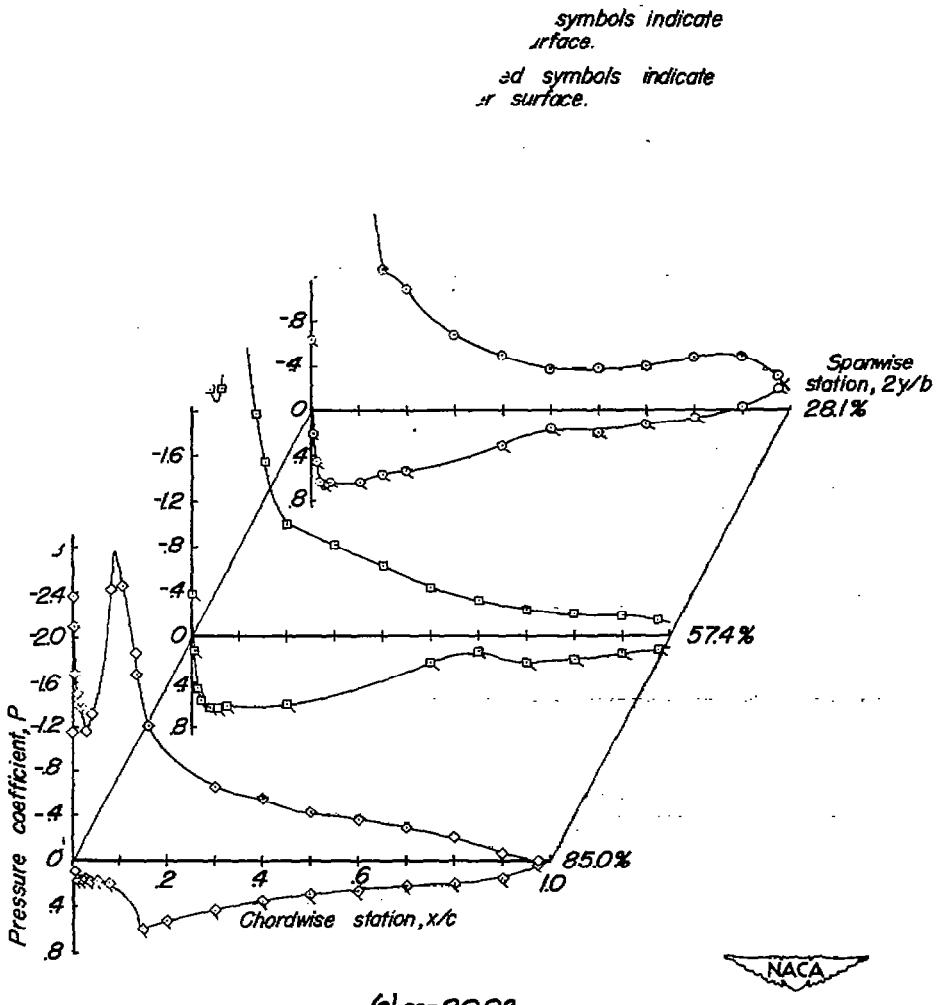

(e) $\alpha = 20.8°$.

Figure 8.–Continued.

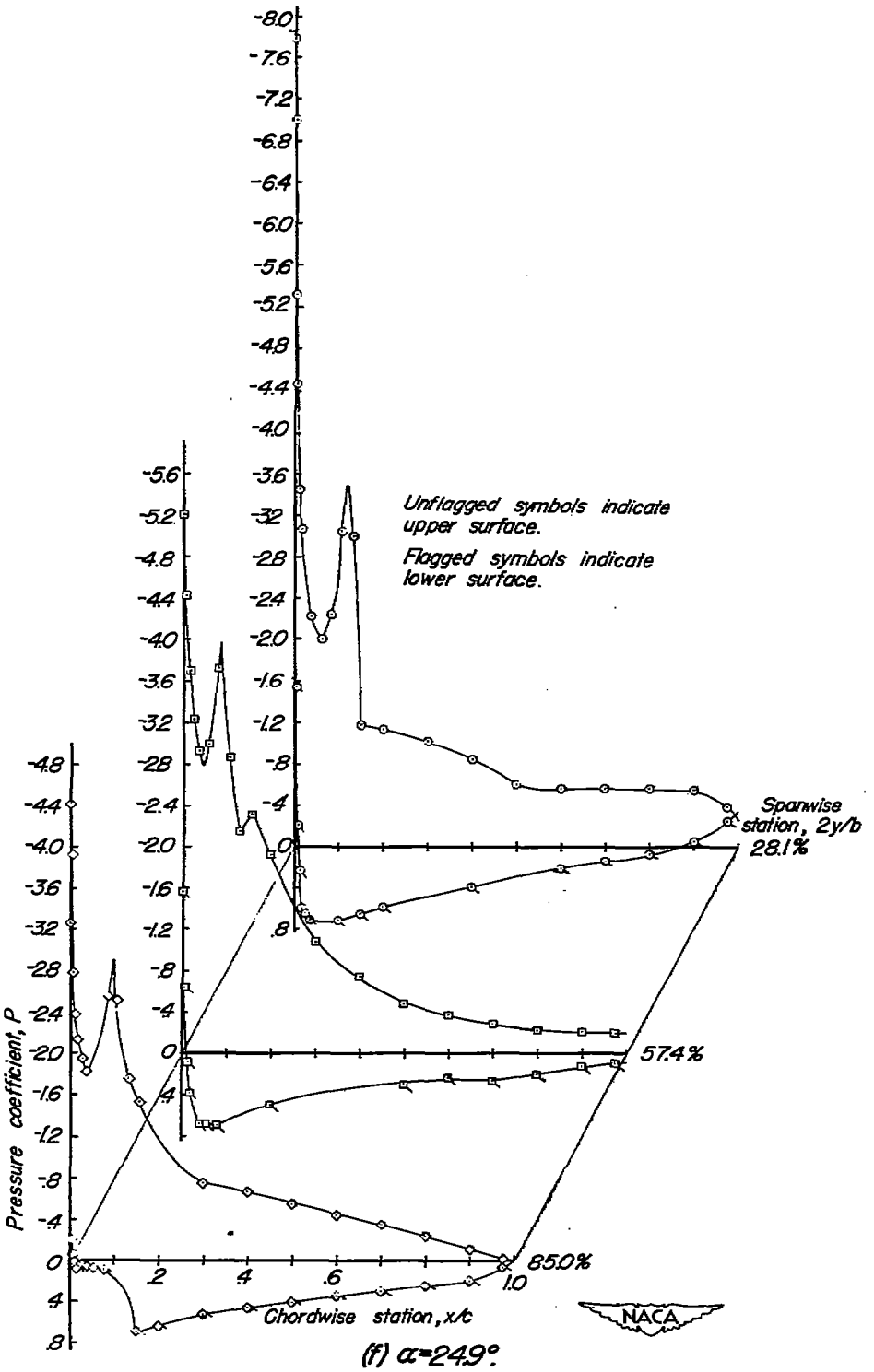

(f) $\alpha = 24.9°$.

Figure 8. –Continued.

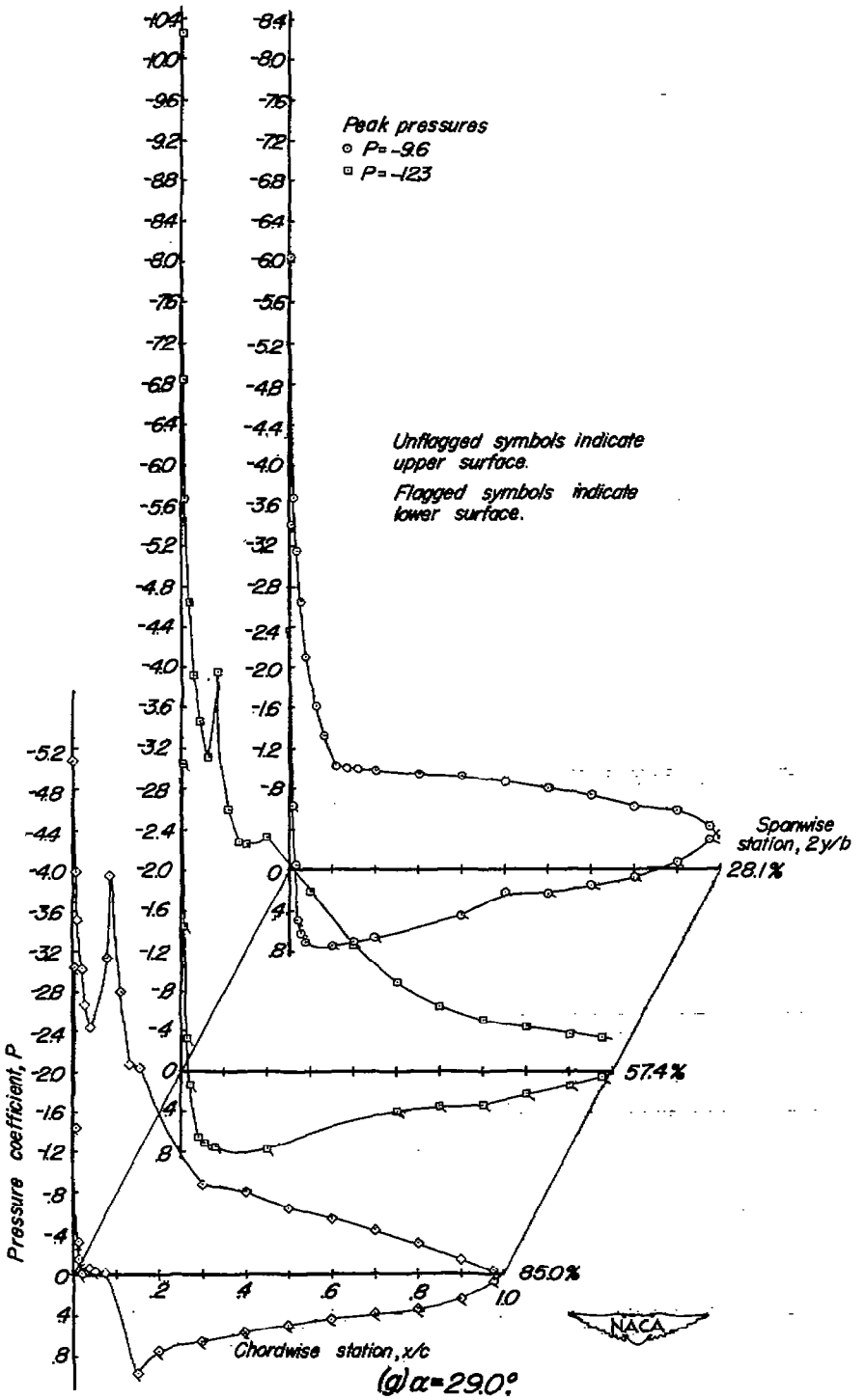

Figure 8.—Concluded.

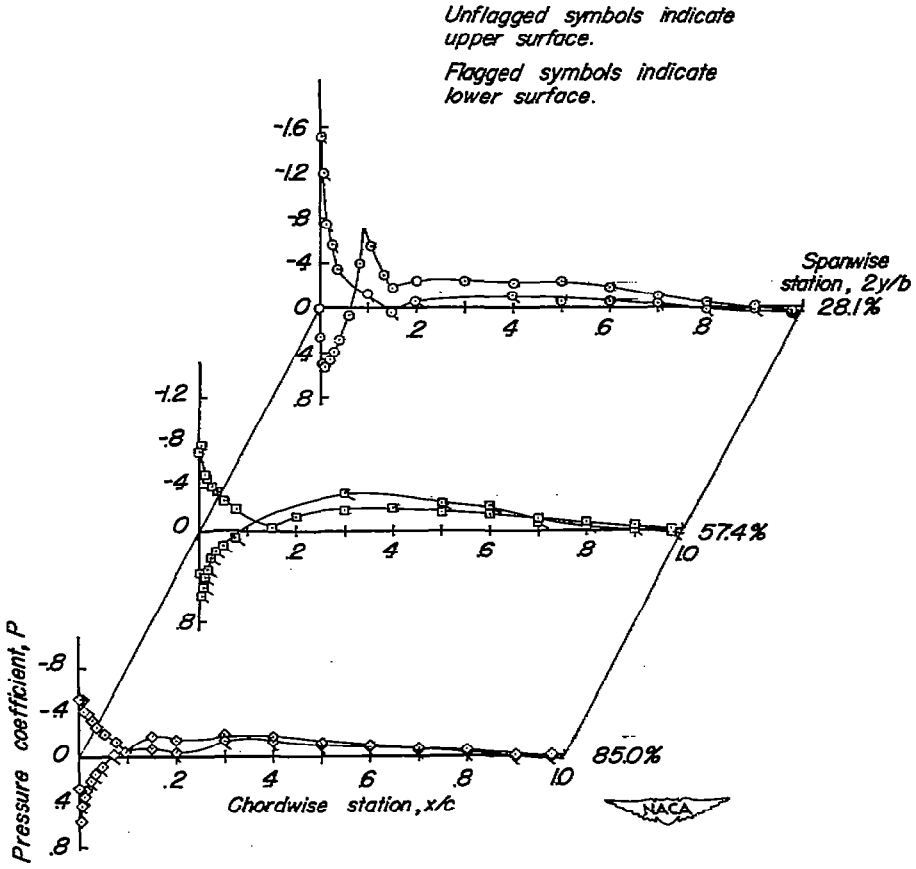

(a) $\alpha = 0.1°$

Figure 9.—Chordwise pressure distributions for 45° swept-forward wing with the inboard half span of leading-edge flap deflected 30° down and the outboard half span deflected 10° up.

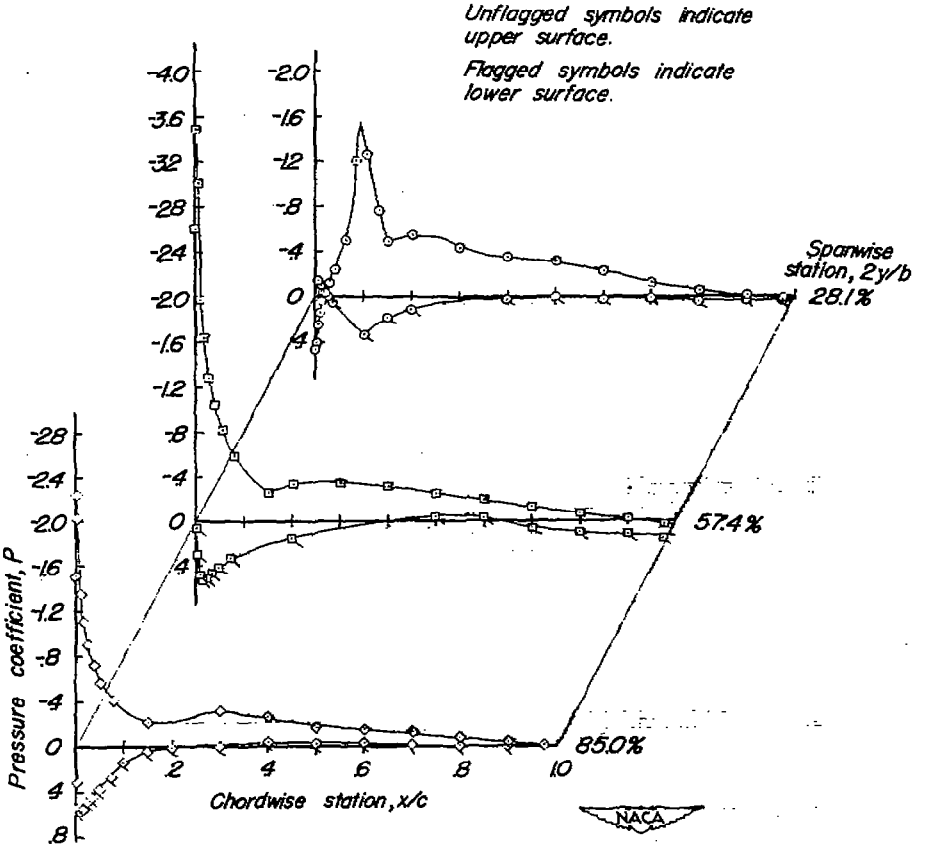

(b) α=6.3°.

Figure 9.-Continued.

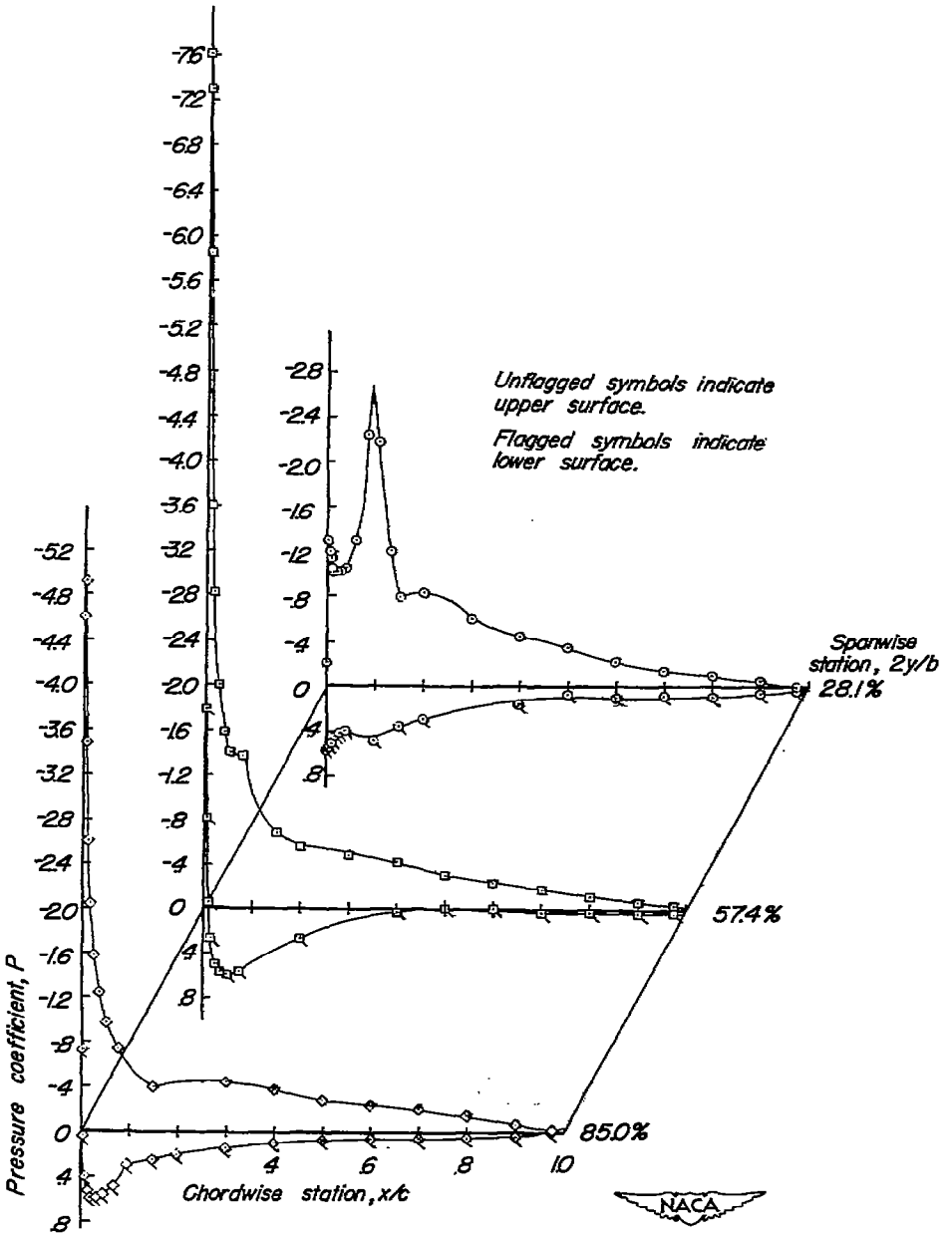

(c) α=12.5°.

Figure 9.– Continued.

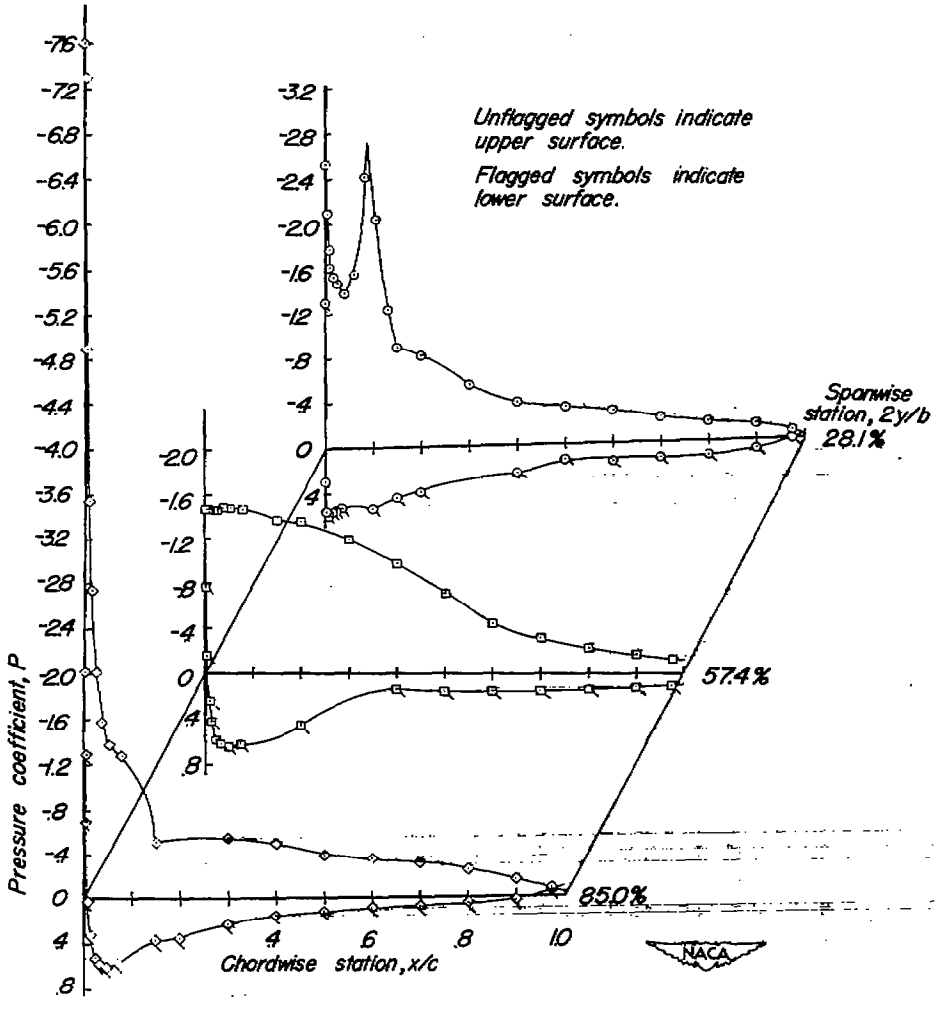

(d) α=16.6°.

Figure 9. – Continued.

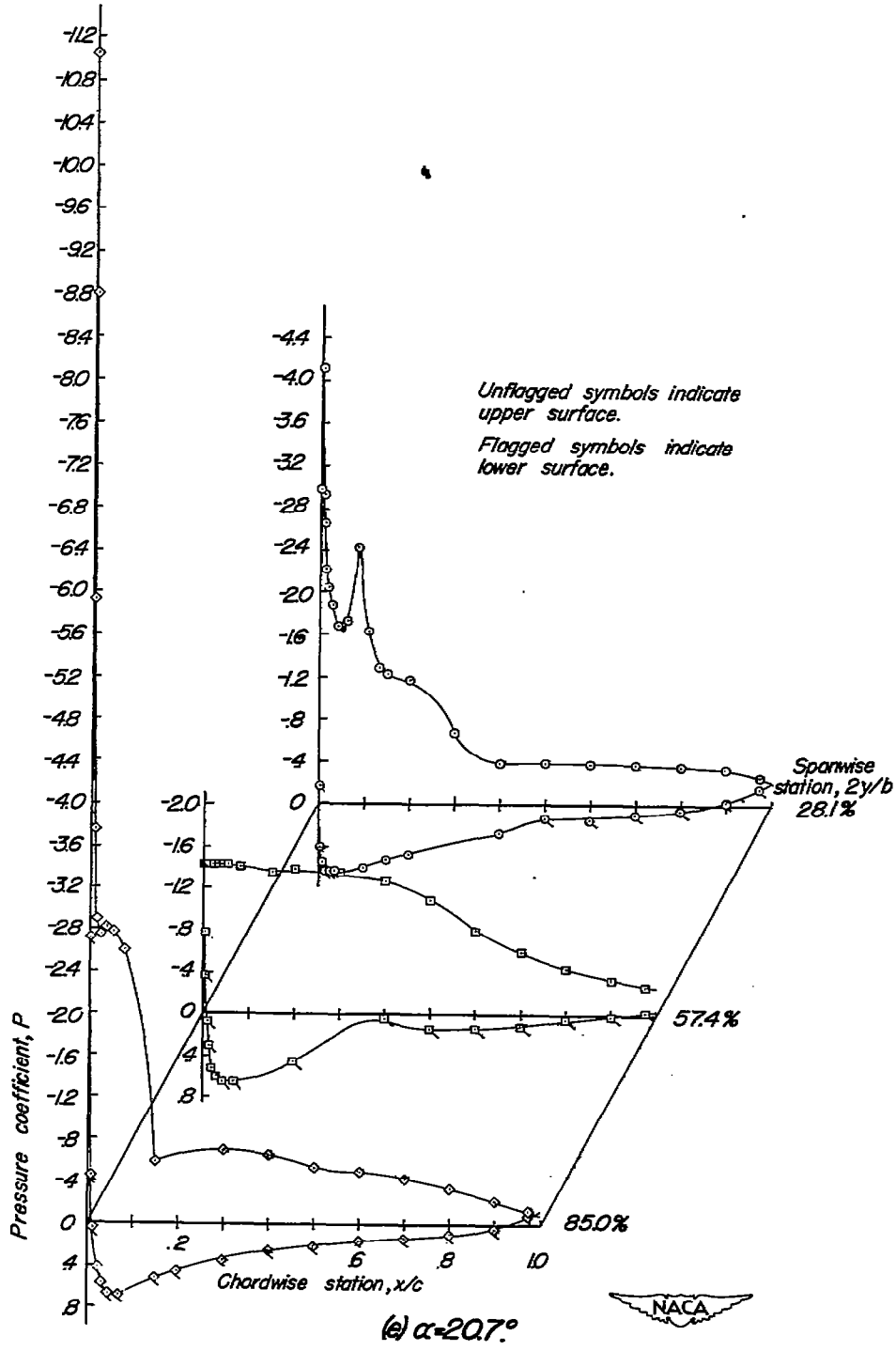

Figure 9. –Continued.

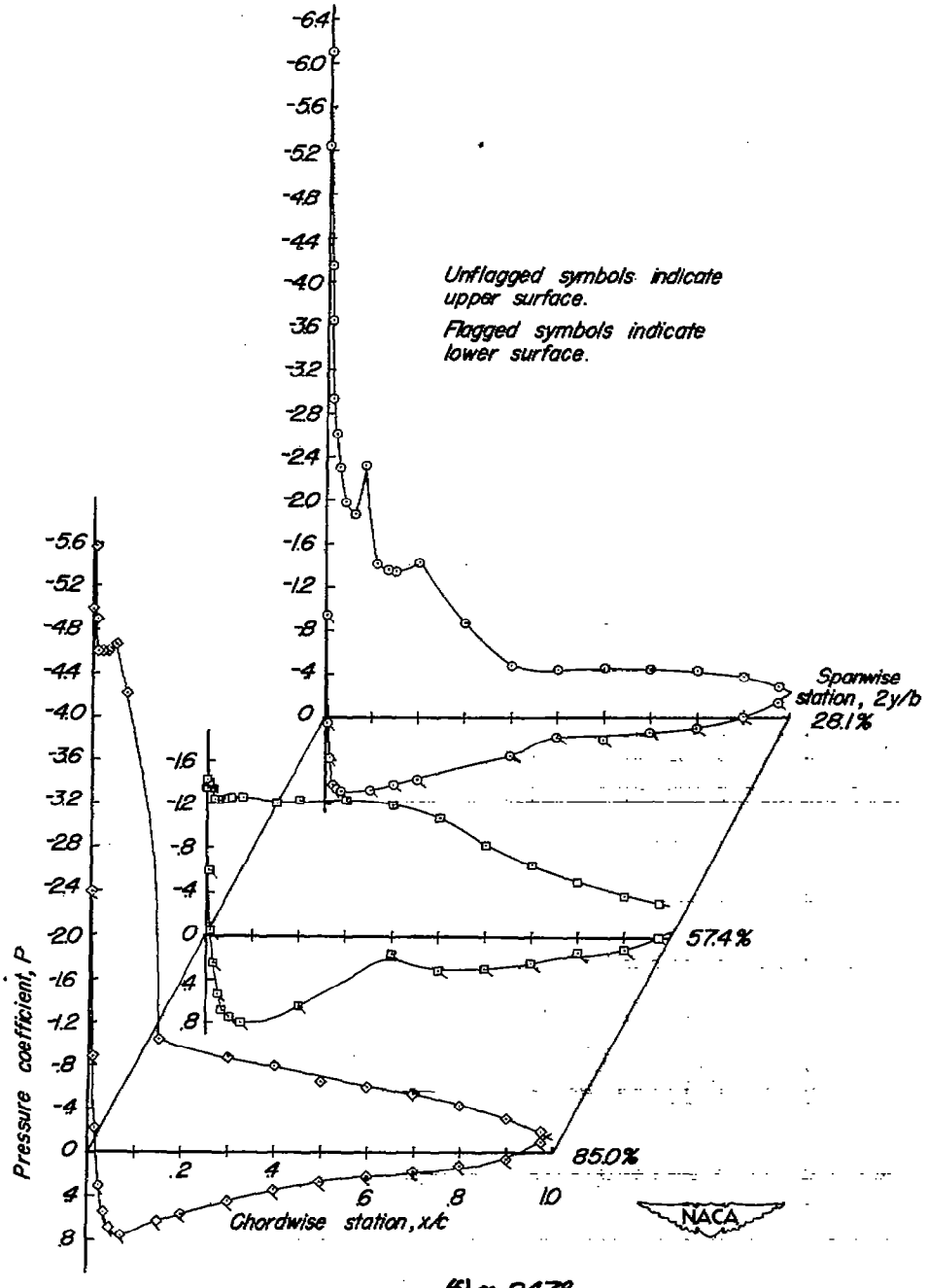

(f) α=24.7°.

Figure 9.–Continued.

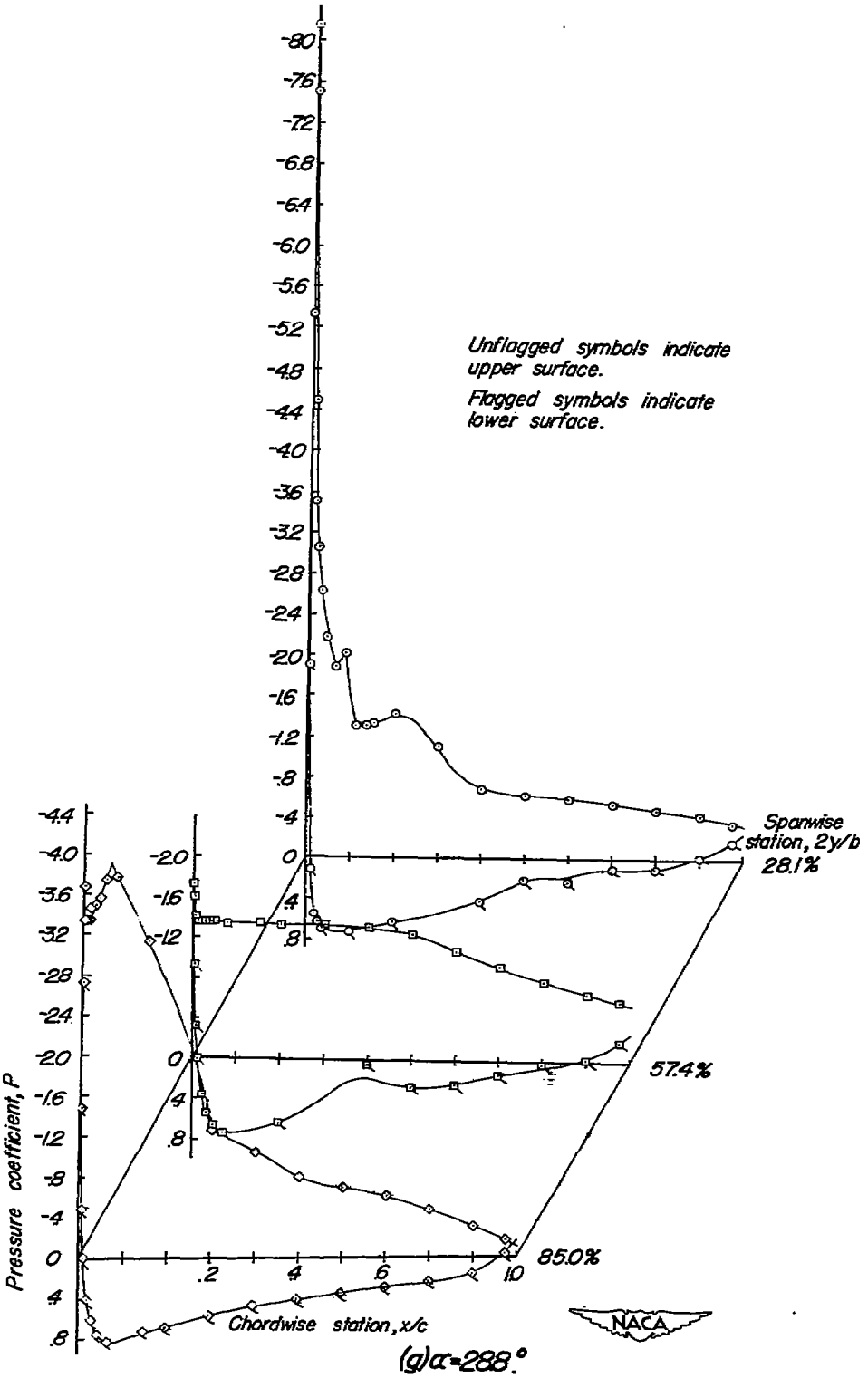

Figure 9.–Concluded.

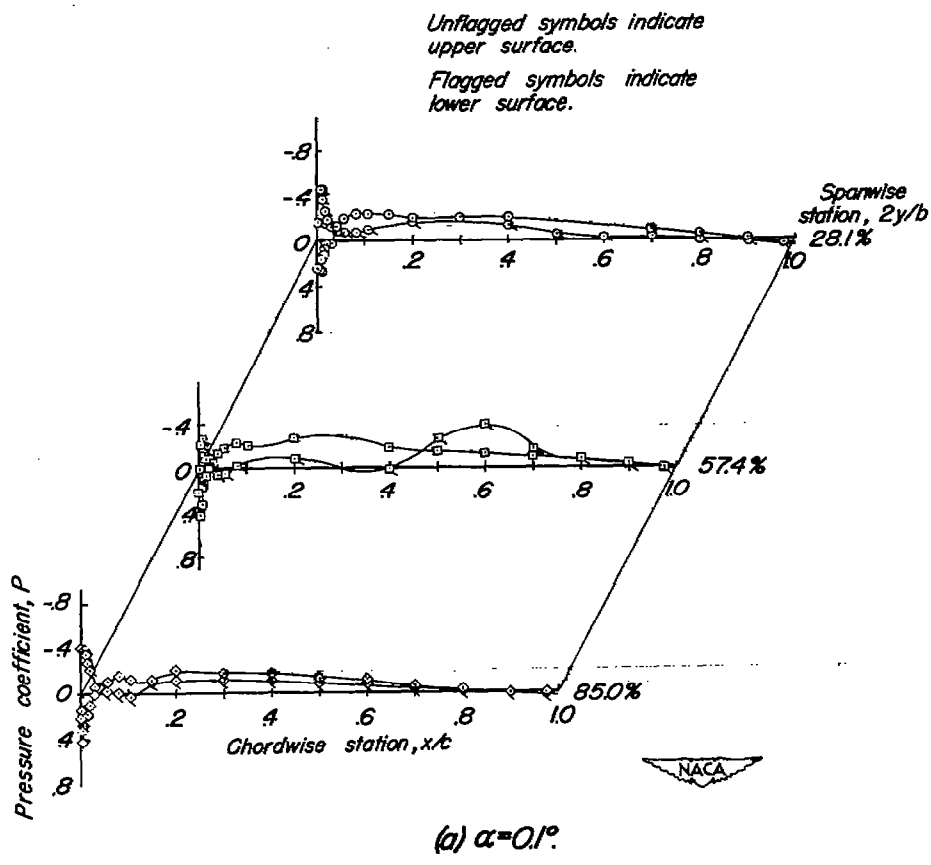

(a) $\alpha = 0.1°$.

Figure 10.-Chordwise pressure distributions for 45° swept-forward wing with a cambered nose.

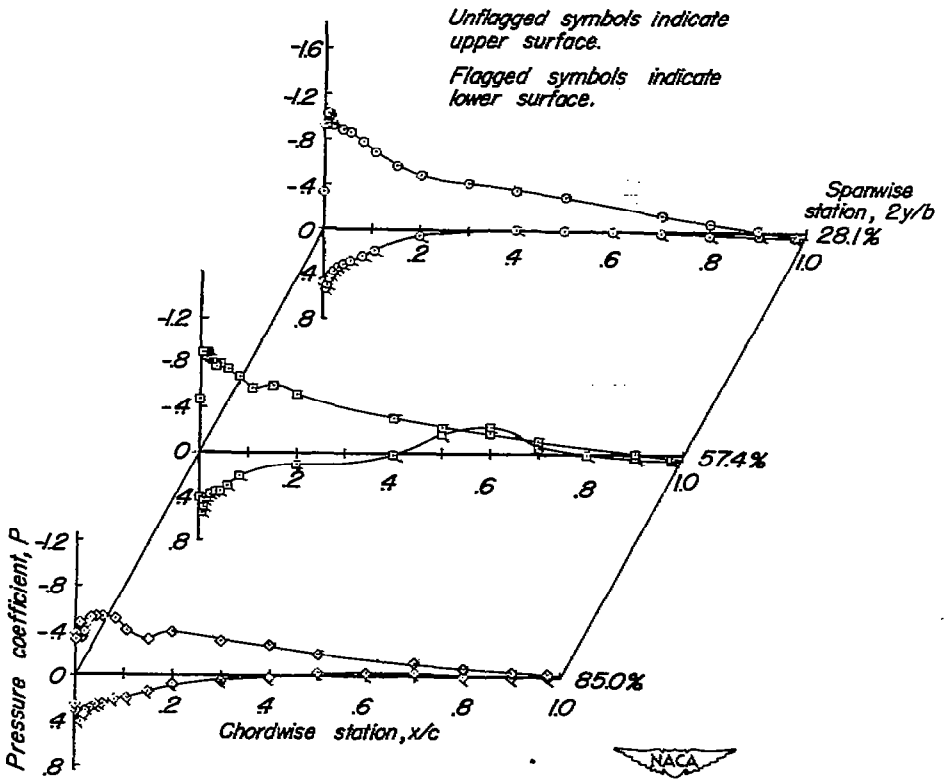

(b) $\alpha = 6.3°$

Figure 10.–Continued.

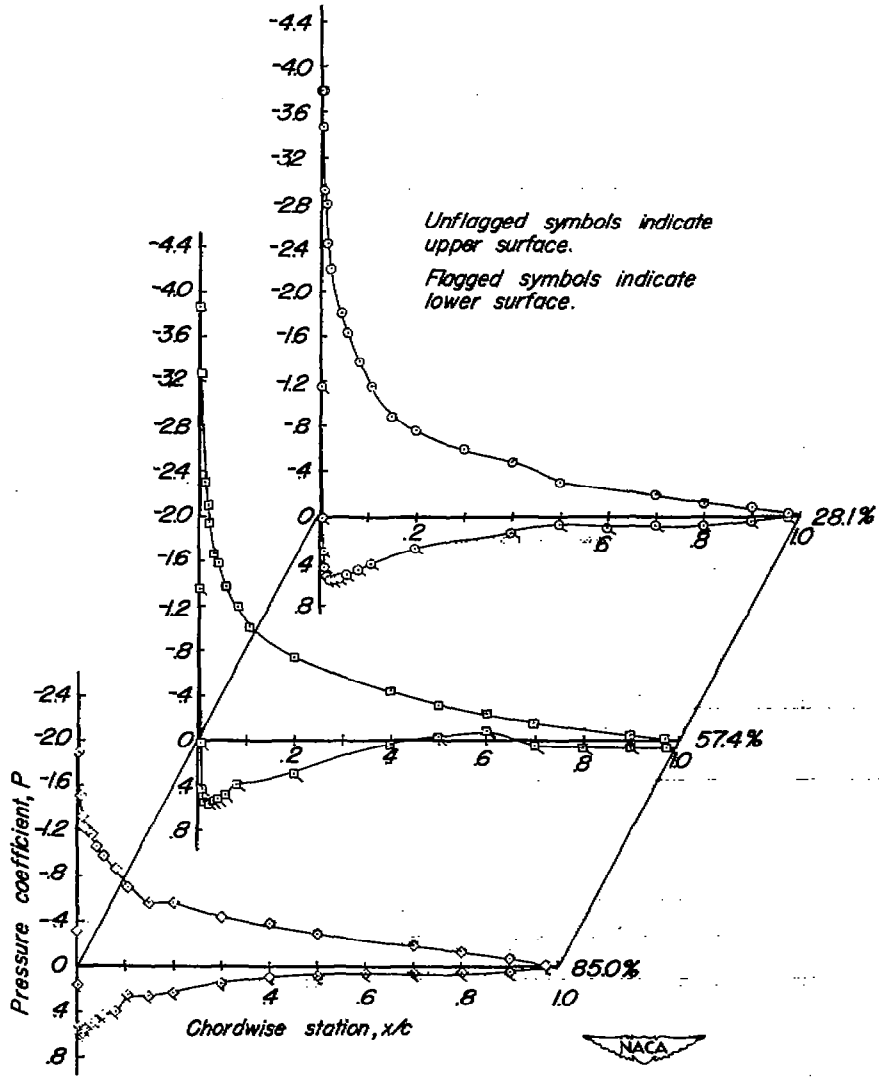

(c) α=12.5°.

Figure 10.–Continued.

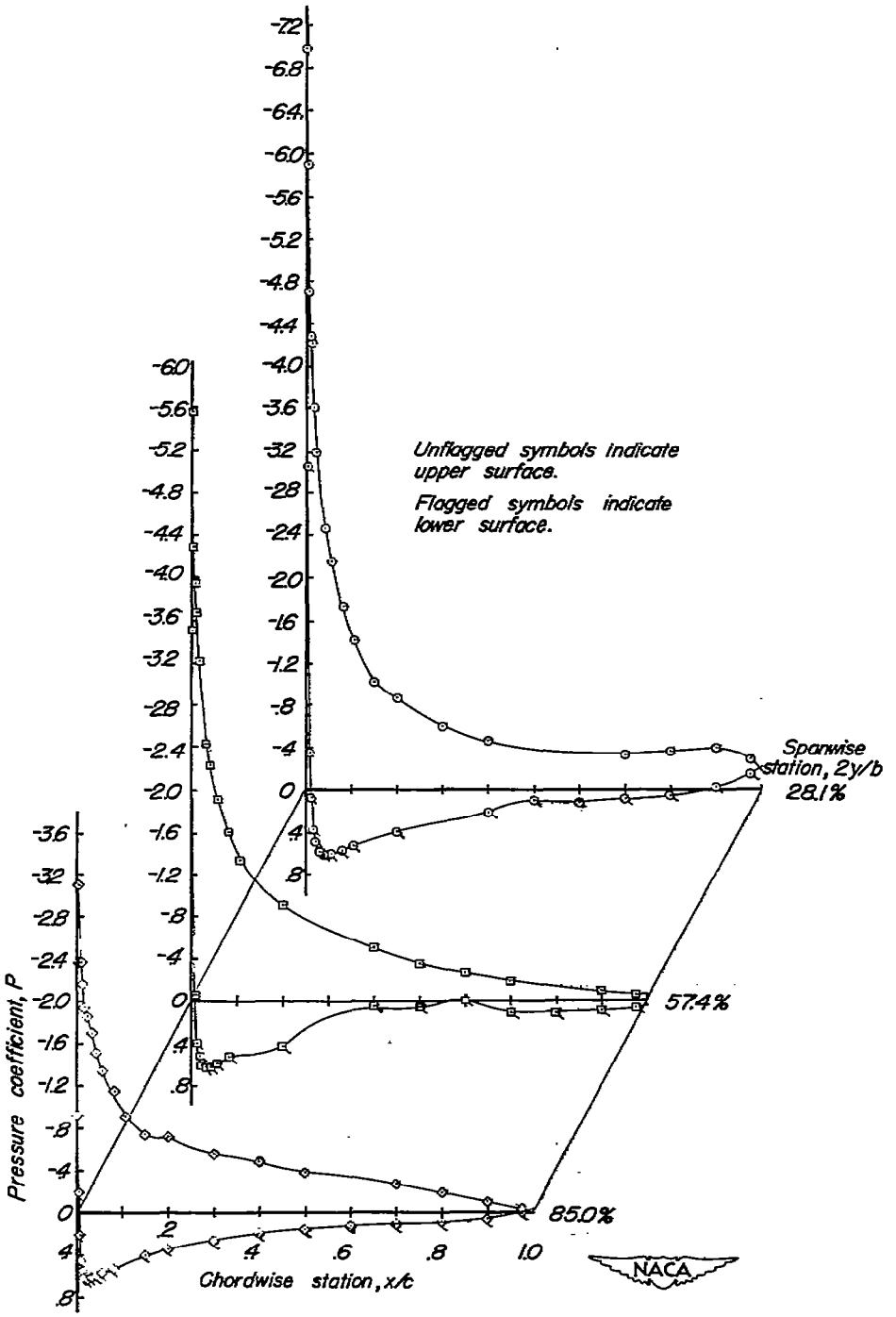

(d) α=16.6°.

Figure 10.- Continued.

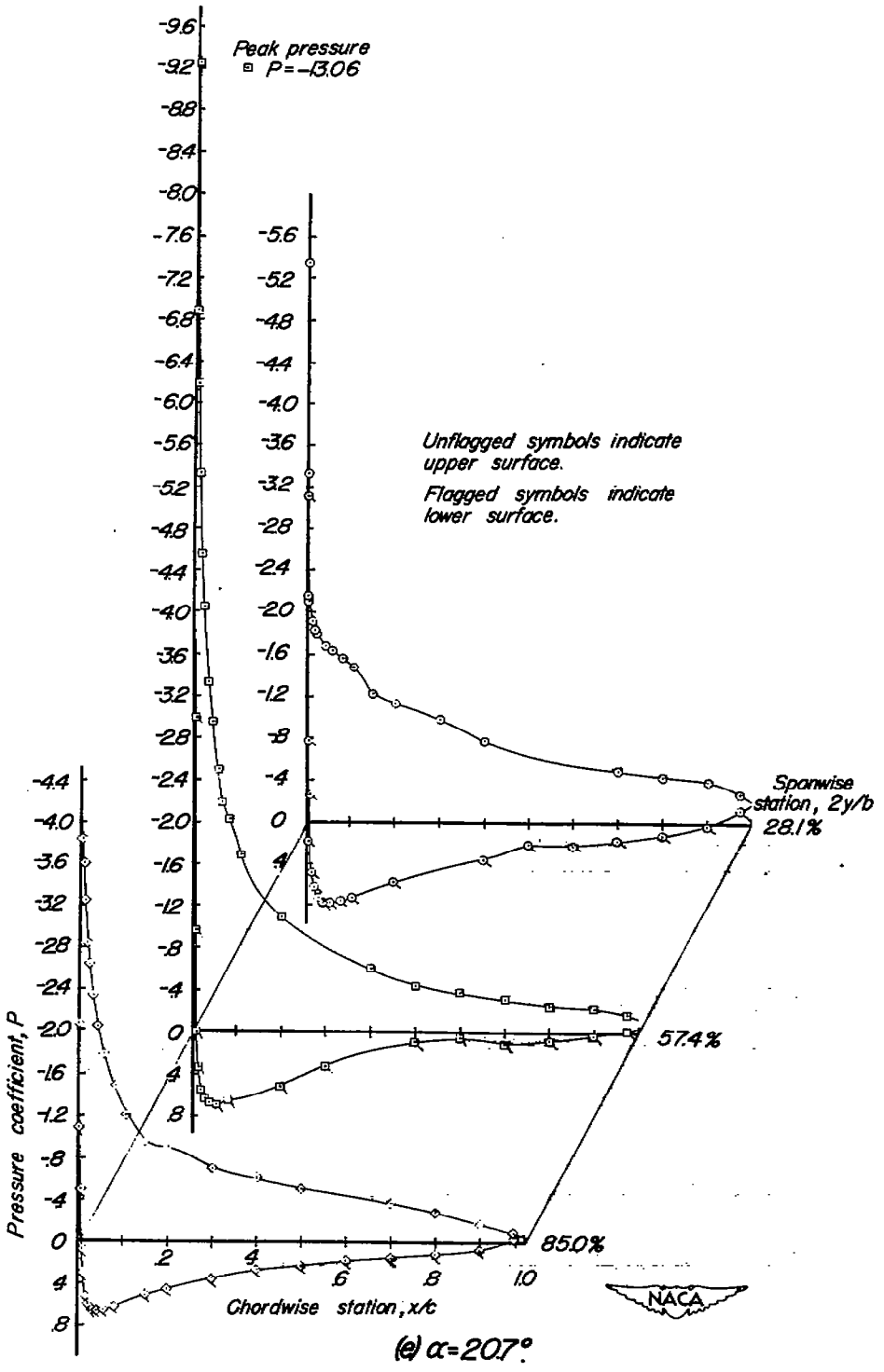

(e) $\alpha = 20.7°$.

Figure 10.–Continued.

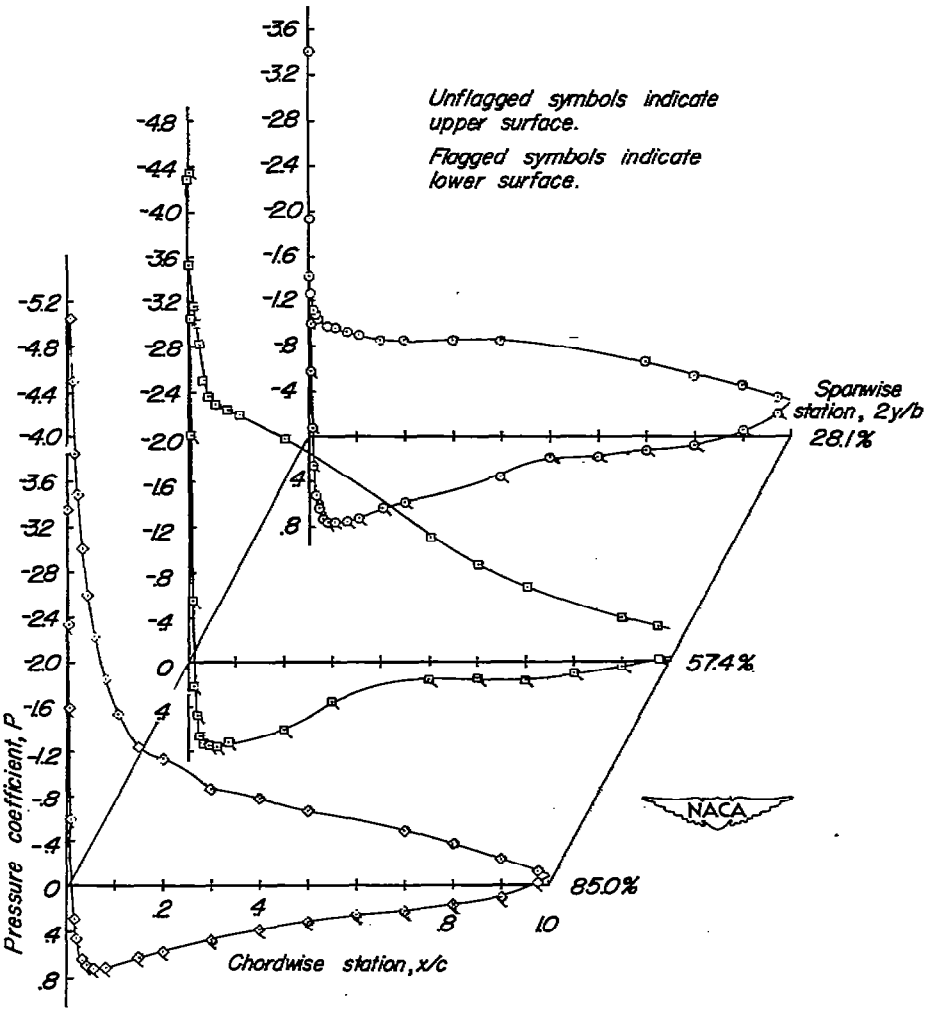

(f) α=24.8°

Figure 10.–Continued.

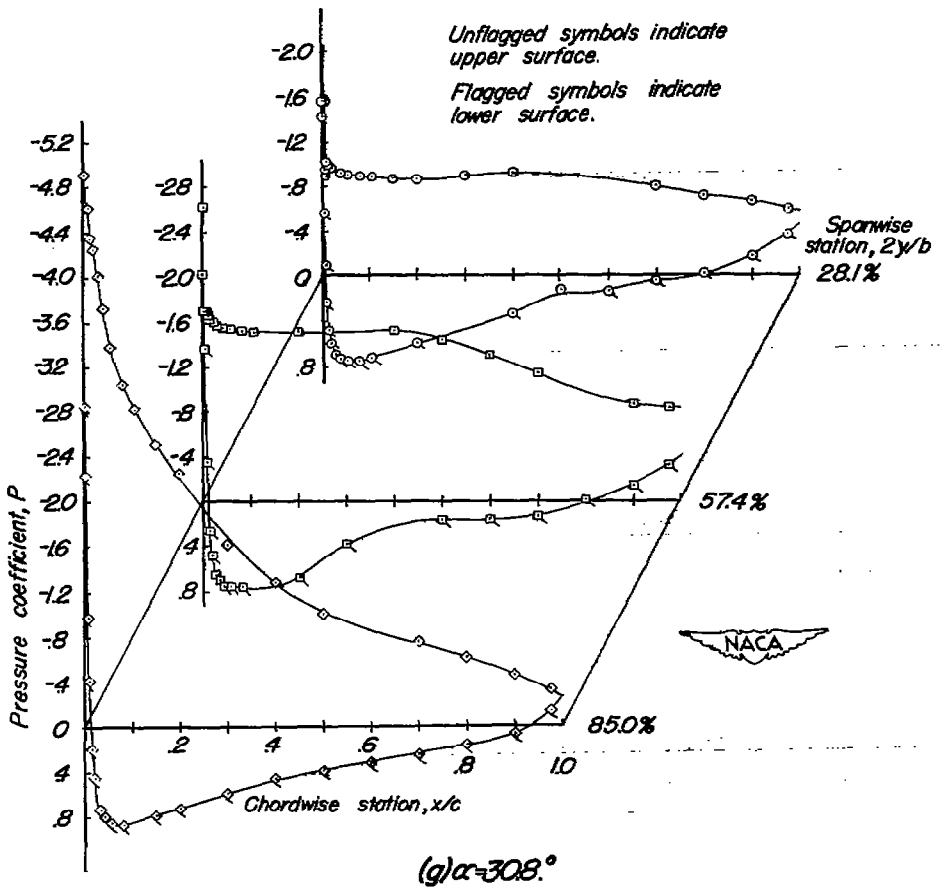

Figure 10.–Concluded.

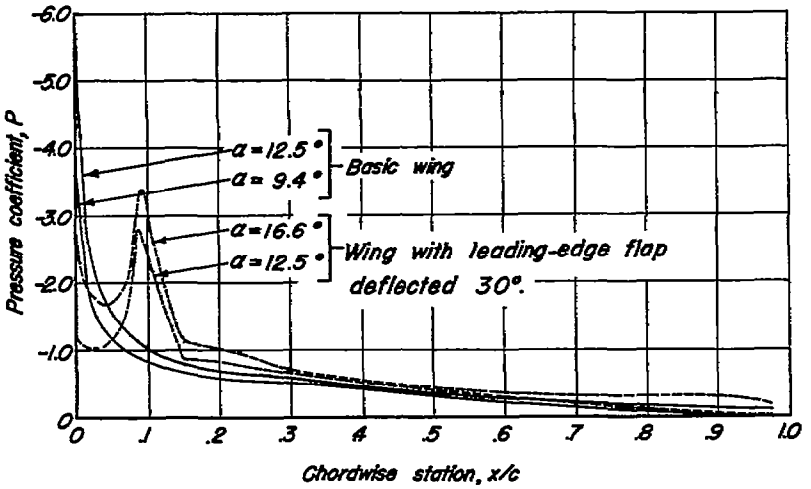

(a) Effects of turbulent separation.

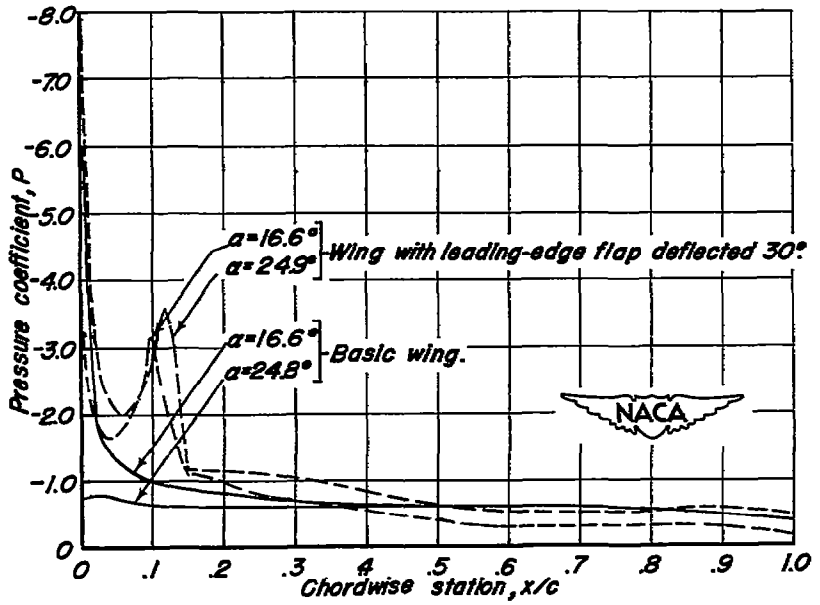

(b) Effects of leading-edge separation.

Figure 11.- Comparisons between upper-surface pressure distributions of basic wing and wing with full-span leading-edge flap deflected 30° down showing the effects of separation over the streamwise section at 28.1% semispan.

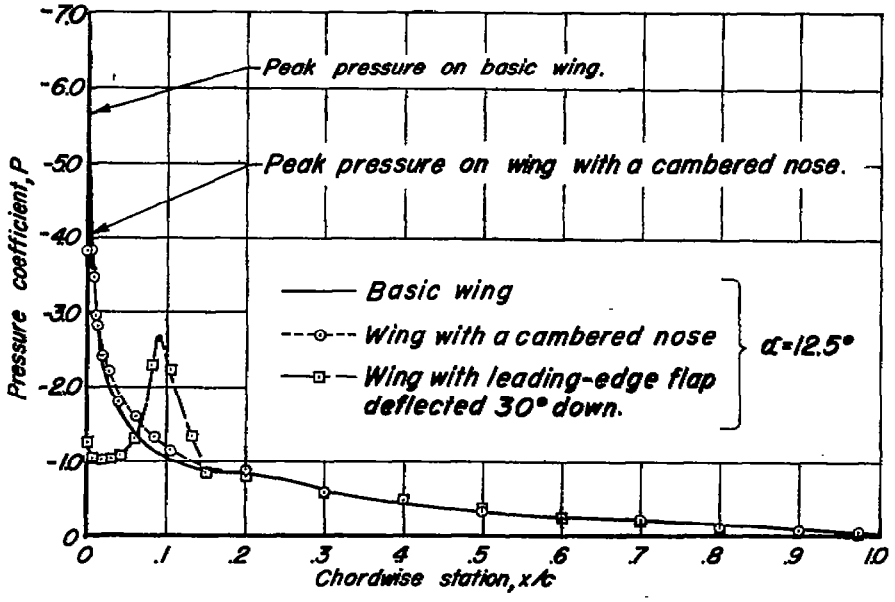

(a) Experimental pressure distributions over section at 28.1 % semispan.

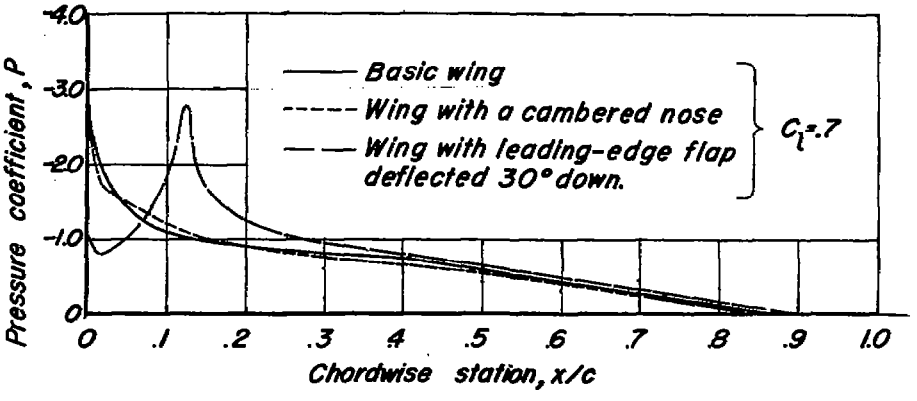

(b) Theoretical pressure distributions.

Figure 12.– Comparisons between upper-surface pressure distributions of basic wing, wing with full-span leading-edge flap deflected 30° down, and wing with full-span cambered nose.